1   **Intercomparison of detection and quantification methods for methane emissions from**
2   **the natural gas distribution network in Hamburg, Germany**

4   Hossein Maazallahi[1,2], Antonio Delre[3], Charlotte Scheutz[3], Anders M. Fredenslund[3], Stefan
5   Schwietzke[4], Hugo Denier van der Gon[2], Thomas Röckmann[1]
6
7   [1]*Institute for Marine and Atmospheric research Utrecht (IMAU), Utrecht University (UU),*
8   *Utrecht, The Netherlands*
9   [2]*Netherlands Organisation for Applied Scientific Research (TNO), Utrecht, the Netherlands*
10 [3]*Department of Environmental Engineering, Technical University of Denmark (DTU),*
11 *Lyngby, Denmark*
12 [4]*Environmental Defense Fund (EDF), Berlin, Germany*
13
14 **Correspondence**: Hossein Maazallahi (h.maazallahi@uu.nl)

Abstract:

17 In August and September 2020, three different measurement methods for quantifying methane
18 (CH_4) emissions from leaks in urban gas distribution networks were applied and compared in
19 Hamburg, Germany: the "mobile", "tracer release" and "suction" methods.
20 The mobile and tracer release methods determine emission rates to the atmosphere from
21 measurements of CH_4 mole fractions in the ambient air, and the tracer release method also
22 includes measurement of a gaseous tracer. The suction method determines emission rates by
23 pumping air out of the ground using soil probes that are placed above the suspected leak
24 location. The quantitative intercomparison of the emission rates from the three methods at a
25 small number of locations is challenging because of limitations of the different methods at
26 different types of leak locations.
27 The mobile method was designed to rapidly quantify the average or total emission rate of many
28 gas leaks in a city, but it yields a large emission rate uncertainty for individual leak locations.
29 Emission rates determined for individual leak locations with the tracer release technique are
30 more precise because the simultaneous measurement of the tracer released at a known rate at
31 the emission source eliminates many of the uncertainties encountered with the mobile method.
32 Nevertheless, care must be taken to properly collocate the tracer release and the leak emission
33 points to avoid biases in emission rate estimates. The suction method could not be completed
34 or applied at locations with widespread subsurface CH_4 accumulation, or due to safety
35 measures. While the number of gas leak locations in this study is small, we observe a
36 correlation between leak emission rate and subsurface accumulation. Wide accumulation
37 places leaks into a safety category that requires immediate repair so that the suction method
38 cannot be applied to these larger leaks in routine operation. This introduced a sampling bias
39 for the suction method in this study towards the low-emission leaks, which do not require
40 immediate repair action. Given that this study is based on random sampling, such a sampling
41 bias may also exist for the suction method outside of this study. While an investigation of the
42 causal relationship between safety category and leak size is beyond the scope of this study, on
43 average higher emission rates were observed from all the three measurement-based
44 quantification methods for leaks with higher safety priority compared to the leaks with lower
45 safety concern. The leak locations where the suction method could not be applied were the
46 biggest emitters as confirmed by the emission rate quantifications using mobile and tracer
47 methods and an engineering method based on leak's diameter, pipeline overpressure and depth
48 at which the pipeline is buried. The corresponding sampling bias for the suction technique led
49 to a low bias in derived emission rates in this study. It is important that future studies using the

50 suction method account for any leaks not quantifiable with this method in order to avoid biases,
51 especially when used to inform emission inventories.
52

1 Introduction

54
55 Natural gas combustion has a lower carbon footprint than combustion of other fossil fuel
56 sources for the same thermal output (EIA, 2021). However, fugitive methane (CH_4) emissions
57 can significantly turn the balance in terms of climate impact (Alvarez et al., 2012) because the
58 global warming potential of CH_4 over a 20-year time scale is 84 times higher than that of carbon
59 dioxide (CO_2) (Myhre et al., 2013). The atmospheric abundance of CH_4 has increased about
60 2.5-fold since the pre-industrial era (Bousquet et al., 2006). Following a short period of stable
61 levels after the year 2000, atmospheric CH_4 has continued to increase since 2006. Worden et
62 al (2017) concluded that about 50 to 80% of the post-2006 increase originated from fossil
63 sources and Jackson et al. (2020) attributed the accelerated increase of $6 - 13$ ppb yr^{-1} from
64 2014 to 2017 (Nisbet et al., 2019), equally to the emission increase from fossil and agriculture
65 sectors.
66
67 Gas distribution networks in cities are subject to maintenance programs by the operators to
68 detect and fix leakages that occur, as CH_4 is an incendiary gas and can be explosive at mixing
69 ratios between 4 and 16% in ambient air (DVGW, 2022). Since the safe operation of the
70 distribution network and leak repair is the primary objective of this maintenance, quantification
71 of emissions from leakages is rarely performed. The absence of regulations on CH_4 emissions
72 is another reason why leak rates are not routinely quantified, however CH_4 emissions from the
73 energy sector need to be addressed properly within the EU CH_4 strategy by 2050 (EC, 2020).
74 Nevertheless, from the perspective of climate change and possible mitigation options, it is
75 important that emissions from gas leakages are (i) quickly detected and fixed and (ii) well
76 quantified. Weller et al. (2020) and Alvarez et al. (2018) respectively reported 5 and 1.6 times
77 higher CH_4 emissions from leaks in the US gas distribution network based on such observations
78 compared to the national inventory reports.
79
80 Leaks from buried pipelines can be due to corrosion or failure/defects in joints or materials
81 (EPA, 1996). When a leak occurs on a buried urban gas pipeline, the gas will generally
82 accumulate in the air space below the surface and then find its path to the atmosphere through
83 a single or several surface outlets. The outlets can be either unpaved soil surfaces, cracks in the
84 road or pavements, or associated with different types of cavities (manholes, communication
85 covers, rain drains, etc.). The major outlet is generally the one with the highest overall
86 permeability for gas released from the buried natural gas pipeline. On the way from the leak
87 location on a buried pipeline to the atmosphere through outlets, CH_4 may be oxidized by
88 methanotrophs in the soil and/or merge with CH_4 from other sources, e.g. biogenic CH_4
89 emissions from sewage systems.
90
91 Routine leak surveys in Germany are conducted by walking with handheld CH_4 sensors above
92 buried pipelines, referred to as the carpet method (DVGW, 2019). The success of leak detection
93 with the carpet method depends primarily on soil permeability (Ulrich et al., 2019), which is
94 influenced by soil moisture, texture, soil organic content and the location of the groundwater
95 table (Wiesner et al., 2016). Based on risk of explosion, gas leaks are classified into four types:
96 A1, A2, B and C (DVGW, 2019). This classification is based on the accumulation of CH_4 in
97 cavities (e.g. manholes, rain drains, etc.) or buildings and the distance of gas leaks to buildings
98 and cavities. If natural gas leaks into buildings or cavities, the leak classifies as A1, and it must

99   be repaired immediately to minimize explosion risk. If the gas leak has a distance up to 1 m to
100 buildings and does not fill cavities, it is classified as A2, and it must be fixed within a week. If
101 the distance is between 1 to 4 m to buildings, the leak is classified as B and the repair time
102 window is three months, and if the distance is more than 4 m then, the leak is considered as C
103 category and can be fixed according to the scheduled repair plan. There are 6,500 km of low
104 pressure and 250 km of medium pressure gas pipelines in Hamburg which are monitored every
105 4 years with the carpet method based on the national regulations in Germany. Gas leaks in
106 cities are not quantified and thus also not a parameter affecting the course of action. Moreover,
107 high pressure pipelines are monitored on an annual basis with additional helicopter-based
108 measurement platforms.

110 In recent years, mobile measurement methods using vehicles with fast and high-precision laser
111 instrumentation have been established for leak detection and emission quantification in
112 numerous cities (Jackson et al., 2014; von Fischer et al., 2017; Weller et al., 2018; Keyes et al.,
113 2020; Ars et al., 2020; Maazallahi et al., 2020; Defratyka et al., 2021; Luetschwager et al.,
114 2021; Fernandez et al., 2022). In-situ measurements of atmospheric CH_4 from mobile vehicles
115 are used to pinpoint and quantify CH_4 emission sources at street level in urban areas. The
116 mobile method was calibrated using above-ground controlled release experiments, in which
117 known amounts of CH_4 were released from gas cylinders (Weller et al., 2019). Simultaneous
118 measurements of carbon dioxide (CO_2) and ethane (C_2H_6) can provide valuable additional
119 information for attributing CH_4 sources (Maazallahi et al., 2020). A characteristic of the
120 resulting emissions distribution from gas distribution grids in cities is the existence of a few
121 leak locations with very high leak rates, up to 100 L min^{-1}, resulting in a right-skewed leak
122 emission rate distribution (Weller et al., 2020). Usually about 10% of the leaks are responsible
123 for between 30% to 70% of the emissions (Weller et al., 2019; Maazallahi et al., 2020).
124 Therefore, the CH_4 emission from the gas distribution system can be reduced very effectively
125 if the largest leaks can be found and fixed quickly, thus augmenting the routine leak detection
126 (carpet method) and repair programs with the mobile method.

128 The tracer dispersion method is another method to quantify CH_4 emissions from point and area
129 sources. In this method, a tracer gas is released at a known rate close to the outlet of the gas
130 leak, and both tracer and target gas mixing ratios are measured downwind. From these
131 measurements and the known tracer gas release rate, the target gas emission rate can be
132 determined with an uncertainty of $\pm$ 15% (Lamb et al., 1995) or less than 20% (Fredenslund et
133 al., 2019). Lamb et al. (2015) applied the tracer method to quantify leaks from urban
134 underground pipelines where they reported moderate agreement ($\pm$ 50%) to excellent
135 agreement ($\pm$ 5%) between the tracer and high-flow sampler method. In the high-flow sampler
136 method, air was drawn at a flow rate of about 0.2 m^3 min^{-1} through a flexible enclosure which
137 covered a leak from a component completely. In this method, CH_4 mixing ratio was measured
138 with catalytic oxidation and thermal conductivity hydrocarbon sensors and a thermal flow
139 meter was used to determine gas flow.

141 Another approach to quantify underground leak rates from buried gas pipelines is the so-called
142 suction method. In this method air is pumped out of the ground at a known rate via probes
143 surrounding the underground leaks until an equilibrium CH_4 mixing ratio is reached in air out-
144 flow, from which the CH_4 leak rate can be calculated. In Germany, this approach is applied to
145 a limited number of leak locations, which do not have to be repaired immediately or within 1
146 week. Suction measurements normally find leak rates that are < 2 L min^{-1} (E.ON, personal
147 communication, 2020). The reported uncertainty range of this method is $\pm$ 10% based on 23
148 measurements in the 1990s (E.ON, personal communication, 2020). The discrepancy between

149 these rather low leak rates compared to leak rates inferred with the mobile method calls for
150 further investigation, since the suction method is also employed to derive network-wide
151 emission factors for the German country-wide gas distribution network (Federal Environment
152 Agency, 2020).

153

154 Hendrick et al. (2016) used surface flux chamber measurements carried out between 2012 and
155 2014 to estimate gas leak rates from 100 leak locations in the Boston area that were detected
156 using mobile measurements (n = 45) in 2011 from Phillips et al. (2013) and additional locations
157 from later mobile surveys (n = 55). They reported CH_4 emission rates from gas leaks ranging
158 from 0.003 g min^{-1} to 16 g min^{-1}, corresponding to roughly 0.0 – 24.4 L min^{-1}. They also
159 reported that their estimate using chamber measurements underestimated total CH_4 emissions,
160 likely because the chambers didn't capture the total CH_4 emitted from the leak. This is similar
161 to the enclosure measurements results from Weller et al. (2018).

162

163 The flow through a hole in a pipeline can also be calculated theoretically and empirically from
164 the physical properties of the hole, mainly the ratio of hole to pipeline diameter and the
165 overpressure in the pipeline. There are three different engineering model types to estimate
166 emissions from gas leaks: the hole model, the rupture model and modified models to bridge the
167 gap between hole and rupture models (Hu et al., 2020; Moloudi and Esfahani, 2014; Yuhua et
168 al., 2002; Arnaldos et al., 1998). These types of models are either to estimate leak strength from
169 a pipeline in open space or a buried pipeline. A leak on a buried pipeline has higher surrounding
170 resistance depending on soil conditions compared to a situation where the pipeline is in open
171 space. Such models have been used to quantify emissions from holes in pipelines in open space
172 (Hou et al., 2020; Manda and Morshed, 2017; Moloudi and Esfahani, 2014; Mahgerefteh, Oke
173 and Atti, 2005; Yuhua et al., 2003; Kayser and Shambaugh, 1991) but also from buried
174 pipelines (Liu et al., 2021; Ebrahimi-Moghadam et al., 2018; Okamoto and Gomi, 2011; Yan,
175 Dong and Li, 2015). Cho et al. (2021) introduced a model, which takes into account soil
176 properties including absolute and relative permeability and porosity, the underground spread
177 of the leak, surface CH_4 mole fractions and depth of the buried pipeline based on experiments
178 with a controlled release rate. This model was calibrated based on release rates ranging from
179 1.3 g min^{-1} to 5.7 g min^{-1}, corresponding to roughly 2.0 – 8.7 L min^{-1}.

180

181 In this study, we present results from measurements with the mobile, the tracer release and the
182 suction methods in Hamburg, Germany, in August and September 2020. We present the
183 quantitative emission estimates as well as a qualitative intercomparison of the three methods,
184 in particular related to the applicability and the strengths and weaknesses of the different
185 methods at different leak locations. We investigate differences between the leaks detected from
186 mobile measurements and leak locations reported from the routine leak detection surveys
187 performed by the local gas utility (hereinafter LDC (Local Distribution Company)). Finally,
188 we discuss implications of our study for national emission inventories.

189

2 Materials and Methods

190

2.1 Campaign preparation and general overview

191
192 As a preparation for the intercomparison campaign, all partners contributed to the preparation
193 of an "intercomparison matrix" where the characteristics and deployment details of the
194 different methods were specified. This matrix is provided in section S.1 of the Supplemental
195 Information (SI). The matrix includes descriptions related to the identification of gas leaks, the
196 quantification of gas leaks, adjustments of the method to the intercomparison exercise and

197 upscaling. It also laid out an initial plan for the intercomparison in terms of identification of
198 suitable locations and deployment of the different methods.
199 According to this plan (Fig. 1), we first applied the mobile method to identify potential gas leak
200 locations, namely leak indications (LIs). When the mobile method had detected one or more
201 emission outlets (See Sect. S.2 in SI) and classified them as a potential gas leak location, the
202 carpet method was applied to confirm the leak and determine the confine leak location. Some
203 additional locations that had previously been identified by the carpet method (leak categories
204 B and C) were added to the list of target locations.
205 Following leak detection, the mobile quantification method (multiple transects) was applied at
206 all the locations and the tracer and suction methods were applied at the confirmed leak
207 locations, and with some restrictions regarding safety, i.e. time allowed between detection and
208 repair of leaks for different leak types, and method capacities, e.g. time required, labor
209 intensity, logistics. The release location for the tracer quantification method was confirmed
210 based on surface screening using a handled methane analyzer. For comparison of the mobile
211 and tracer release methods with the suction and hole methods we assumed that (i) a steady state
212 between pipeline leakage under-ground CH_4 accumulation and emission to the atmosphere had
213 been reached (Kirchgessner et al., 1997) and (ii) methanotrophs and methanogens have
214 negligible impact on quantification of gas leak emissions. Thus, the total emission rate of all
215 outlets in the vicinity of a leak location is equal to the natural gas emission rate from the
216 pipeline leak. We will discuss implications of the above assumptions for selected cases. After
217 leak repair, the LDC reported leak hole sizes, pipeline diameters and pipeline operational
218 pressures, allowing leak rate estimation with the hole method.

219
220 **Figure 1 – Flowchart of application of leak detection methods (blue colors) and**
221 **quantification methods (red colors) followed by repair actions and intercomparison of**
222 **the detection and quantification methods.**

2.2 Measurements setups

2.2.1 Mobile measurement setup

Onboard the measurement vehicle (VW Transporter) we operated two cavity ring-down spectrometers (CRDS), model G2301 and model G4302 (Picarro, Santa Clara, California, USA). The G2301 measures CH_4, CO_2 and water vapor (H_2O) at a flow rate of ≈ 0.2 L min^{-1} and 0.3 Hz frequency. The G4302 has a flow rate of ≈ 2.2 L min^{-1} and sampling frequency of about 1 Hz for CH_4, C_2H_6 and H_2O. The air intake for both instruments was from the same tubing attached to the front bumper. This setup allowed us to directly compare the enhancements observed from the two instruments during surveys. The G4302, which is in a shape of a backpack, was also used in attribution of outlets emissions in walking surveys to check presence of C_2H_6 in emission outlets.

2.2.2 Tracer release measurement setup

The tracer release method was applied by releasing acetylene (C_2H_2) at the emission outlet identified by the mobile leak detection and confirmed by the carpet method. The tracer gas was released at the main emission outlet, which was confirmed by surface screening using a handheld CH_4 analyzer. Tracer release rates between 1.3 and 2.6 L min^{-1} from a gas cylinder. A Picarro CRDS, G2203 instrument was used to measure CH_4 and C_2H_2 mole fractions continuously with ≈ 0.3 Hz frequency. The instrument was installed in a measurement vehicle (VW Caddy), and air was sampled from the atmosphere through an inlet on the roof about 2m above ground. The tracer method was applied either in static mode, where air was sampled in one or a few locations downwind from the outlets and tracer release locations (n = 11) or mobile mode (n = 5), where the plumes were transected while measuring mixing ratios of CH_4 and C_2H_2. The choice of mode depended on the site conditions including road accessibility and wind direction. The tracer release setup including instrumentation used as well as mobile mode is described in detail in Mønster et al (2014), and the principle of the static mode is described in Fredenslund et al (2010).

2.2.3 Suction measurement setup

In the suction method, 12 probes were used to insert in the soil around the confirmed gas leak location by the LDC. The probes are connected to a pump to extract accumulated subsurface CH_4 from the leak. CH_4 mole fraction at the outflow is measured with a Flame Ionization Detector (MEEM, 2018).

2.2.4 Carpet method setup

Leak detection experts from the LDC operate a methane detector (Sewerin instruments, Gütersloh, Germany) on a rolling device, where a plastic cover (the carpet) moves over the ground and provides a loose seal to the surrounding atmosphere, facilitating preferential analysis of air emanating from the surface right below the carpet. The instrument gives an acoustic signal when a high CH_4 from a potential leak has been detected. The instrument can detect C_2H_6 by gas chromatography in batch mode, which means that after taking air samples from a suspected outlet, the instrument operator needs to wait for couple of minutes to test possible detection of C_2H_6. This is substantially slower than instrument with 1 Hz frequency used in the mobile method.

2.3 Detection, confirmation and attribution of emissions at gas leak locations

2.3.1 Mobile detection of possible leak location

For leak detection with the mobile method, we first evaluated CH_4, C_2H_6 and CO_2 signals during mobile surveys. If (i) CH_4 and C_2H_6 signals were observed with a ratio of less than 10% with no CO_2 signal or (ii) CH_4 was observed (< 500 ppb enhancement on G4302) with no C_2H_6

273 and CO_2 signals, then we parked the mobile measurement car, detached the G4302 analyzer
274 from the system and searched for gas outlets on foot with the G4302. This detailed search for
275 outlets was performed to (i) confirm the presence of both CH_4 and C_2H_6 signals (ii) map the
276 spatial spread of outlets and (iii) spatially constrain the possible gas leak location. The reported
277 possible gas leak locations from the mobile method were then reported to the LDC for
278 confirmation and localization of the leak with the carpet method and subsequent underground
279 measurements.
280
281 **2.3.2 Attribution of leak indication signals from mobile measurements**
282 To attribute an observed leak indication (LI) from mobile measurements to a source category,
283 namely fossil, microbial and combustion, we used CO_2 and C_2H_6 signals, which were
284 continuously measured along with CH_4. We quantitatively evaluated C_2:C_1 ratios (%) when (i)
285 the CH_4 enhancements were larger than 0.5 ppm (ii) C_2H_6 enhancements were also larger than
286 15 ppb and (iii) the determination coefficient (R^2) of the linear regression between CH_4 and
287 C_2H_6 was larger than 0.7. If CH_4 signals in mobile measurements were associated with CO_2
288 and high C_2H_6 mole fractions (C_2:C_1 > 10%), we attributed those emissions to combustion
289 (Maazallahi et al., 2020). When we repeatedly observed CH_4 enhancements, no CO_2
290 enhancements and C_2:C_1 ratios between 1 and 10%, or we observed persistent CH_4 signals in
291 several passes we did further on-foot inspection of the outlets. If the emissions from the outlets
292 clearly pointed to a fossil origin based on the CH_4 and C_2H_6 signals, we labeled the locations
293 as potential gas leak locations and reported them to the LDC for confirmation. We only
294 considered a location as a gas leak for further investigation if the LDC confirmed the existence
295 of a gas leak.
296 If at a particular location, we observed several CH_4 maxima, for example from different outlets,
297 we considered the "strongest" outlet as the main emission point. The "strongest" emission point
298 refers to a point where we observed the highest CH_4 mole fraction when the G4302 intake inlet
299 was put at a distance of $\approx$ 2 - 5 cm above the surface or outlet. When several emission outlets
300 with same order of magnitude in mole fractions were found, we considered the spatial average
301 of the coordinates as the main emission point. The tracer method then released C_2H_2 at the
302 main outlet emission point.
303 The LDC reported a C_2:C_1 ratio of 3.0% (96.20 $\pm$ 0.02 mol % CH_4 and 2.88 $\pm$ 0.00 mol %
304 C_2H_6, GNH personal communication) for the gas composition in the grid for the period of
305 August and September 2020 in Hamburg. This ratio was reported 3.5% (95.09 mol % CH_4 and
306 3.37 mol %, GNH personal communication) in April 2020.
307
308 **2.3.3 LDC leak detection and confirmation**
309 Since the pipeline locations are known to the LDC, the method can be applied precisely above
310 the pipelines, including visible cracks and cavity outlets in the close vicinity, increasing the
311 possibility of leak detection. Once the carpet method detects a CH_4 source, a second
312 measurement is performed above the location with the highest signal, where air is accumulated
313 and analyzed for the presence of C_2H_6. The C_2H_6 detection in the carpet method is not online
314 with higher detection threshold and in batch mode (gas chromatography), which takes time, 5
315 – 10 minutes per location. If sufficiently high CH_4 and C_2H_6 levels are found, the leak is
316 categorized in one of safety categories of A1, A2, B or C.
317
318 **2.3.4 Precise underground leak localization**
319 When a leak has been confirmed with the carpet method, a precise localization of the leak is
320 performed by drilling holes about 20-40 cm into the ground along the pipeline track and
321 measuring the sub-surface CH_4 mixing ratio. The location with the maximum sub-surface
322 reading is assigned the most likely leak location where the repair teams open the road and

attempt repair of the leak. The final exact leak location is reported after opening ground for the repair reactions. Mostly the locations reported from the carpet method matches the locations reported from the leak repair team, which depends on the transport pathways of emission undersurface and surface coverage.

2.4 Emission quantification
2.4.1 Mobile measurements quantifications
After the detection of the target locations, we performed additional transects at these locations on different days. We accepted a mobile measurement transect of a leak location for further analysis if (i) the GPS signals of transects were logged correctly along the street track and (ii) at least one of the two instruments, G2301 (for quantification and attribution) and / or G4302 (for attribution), were running during the transect and (iii) the transect track included at least one GPS coordinate less than 50 m from the leak location. The start and end point of the accepted transects were determined as the locations where the driving tracks intersected with a circle with radius of 100 m centered at the gas leak location reported by the LDC, or a reported outlet location from the mobile method, for the locations where the LDC did not confirm a leak. The segments between the start and end points were evaluated one by one (See an example in Sect. S.4.1 in SI) to determine various parameters, e.g., the maximum CH_4 enhancements, plume area, driving speed, distance to the actual leak locations, etc. The plume area is the integral of the CH_4 enhancements above background along the driving track from the location where the CH_4 enhancement exceeds > 10 ppb until the location where it falls again below the 10 ppb threshold.

Gas leak quantification from mobile measurements is based on an empirical equation derived from controlled release experiments reported by von Fischer et al., (2017) and reevaluated in Weller et al., (2019) (Eq. 1).

$$Q = \exp \left((\overline{Ln \, (C_{max})} + 0.988) / 0.817 \right) \qquad \text{Eq. 1}$$

In Eq. 1, C_{max} is the maximum CH_4 enhancement (ppm) observed during each transect next to the leak location. The maximum CH_4 enhancement should be more than 10% above CH_4 background level to be considered for the quantification algorithm. The emission rate is denoted by Q and it is in L min^{-1}. $\overline{Ln \, (C_{max})}$ is the mean of the logarithm of the maximum mole fraction enhancements for all accepted transects.

The standard quantification method only uses transects where CH_4 enhancements are more than 10% or $\approx$ 200 ppb above background level. This 10% enhancement threshold corresponds to about 0.5 L min^{-1} emission rate in Eq. 1. Thus, $\approx$ 0.5 L min^{-1} is the minimum emission rate that can be quantified with Eq. 1 and leaks with smaller emission rates are ignored by design of the method. Below we investigate the effect of relaxing the enhancement threshold. The application of the tracer release technique in mobile mode allowed us to use the known C_2H_2 release rate and the measured C_2H_2 plumes to independently validate the mobile approach, including the effect of the enhancement threshold. We also investigated the effect of distance between CH_4 maxima to gas leak locations, which is not a parameter in Eq. 1.

The uncertainty of the emission rate for each location in the mobile method was calculated using standard error and t-factor (95% confidence) for the locations with at least three CH_4 enhancements greater than the 10% threshold.

In addition to evaluating the maximum CH_4 enhancement from each transect we also derived the plume area (mixing ratio times distance and in unit of ppm m) for comparison between the instruments. In principle, the plume area should provide a more robust quantification of an ambient CH_4 plume than the maximum enhancement: When a plume spreads out, individual realizations of the plume can be sharper and higher, or wider and lower, depending on

373 meteorological conditions, but the plume area should be less affected. In addition, when an
374 instantaneous plume is sampled with two instruments with different gas flow rates, instruments
375 with a lower flow rate will be affected by mixing of air in the measurement cell. This will lead
376 to a lower maximum enhancement but a wider peak, and thus the peak area should lead to a
377 better comparison between the instruments.
378
379 **2.4.2 Tracer measurements quantifications**
380 The tracer method uses Eq. 2a to quantify CH_4 emissions in mobile mode (integral over space
381 dimension) and Eq. 2b in the static mode (integral over time dimension). Parameters relevant
382 for the evaluation with the tracer method are provided in Sect. S.4.2.

383
$$Q_{CH_4} = Q_{C_2H_2} \cdot \frac{\int_{start}^{end} C_{CH_4} dx}{\int_{start}^{end} C_{C_2H_2} dx} \cdot \frac{MW_{CH_4}}{MW_{C_2H_2}}$$
Eq. 2a

384
$$Q_{CH_4} = Q_{C_2H_2} \cdot \frac{\int_{start}^{end} C_{CH_4} dt}{\int_{start}^{end} C_{C_2H_2} dt} \cdot \frac{MW_{CH_4}}{MW_{C_2H_2}}$$
Eq. 2b

385
386 Here C is the mole fraction (ppm) and MW is the molecular weight of the species, 16 g mol^{-1}
387 for CH_4 and 26 g mol^{-1} for C_2H_2. Q_{CH_4} is the CH_4 emission rate estimate for CH_4 (g s^{-1}) and
388 $Q_{C_2H_2}$ is the controlled release rate of C_2H_2 (g s^{-1}). The C_2H_2 flow rate was controlled and
389 measured with a flow controller (Brooks Sho-Rate). In addition, the mass of C_2H_2 released at
390 each location was measured by weighing the release cylinder before and after the tracer release
391 with a precise scale (KERN DE60K5A). The change in mass was then converted to a mass
392 flow rate using the release time. To convert the emission rate from mass (g s^{-1}) to volume (L
393 min^{-1}) we used normal temperature and pressure (NTP) conditions, T = 293.15 K, p = 1.01325
394 bar. The locations of tracer release (C_2H_2) at the confirmed gas locations were determined with
395 the combined information from the mobile and the carpet methods.
396 The tracer gas can also be used to pinpoint and confirm the emission source location. Prior to
397 quantification, it is important that the emission outlet is located for proper tracer release (see
398 Fig. 1) and source simulation and that other potential interfering emission sources can be ruled
399 out. This is secured by performance of upwind and downwind CH_4 mole fraction screening.
400 During transecting of the CH_4 and tracer plumes, the two plumes should match, if this is not
401 the case, the tracer release should be relocated until a proper plume match is obtained. If an
402 emission source consists of multiple outlets, the combined emission from all outlets can be
403 measured by releasing the tracer at the main outlet and increasing the measuring distance until
404 one confined overlapping plume of CH_4 and tracer gas is obtained. If the distance cannot be
405 increased to access limitations, tracer should be released at each single emission outlet.
406
407 **2.4.3 Suction measurements quantifications**
408 The quantification of a leak with suction method is possible after pumping accumulated air out
409 of soil and reaching CH_4 mole fraction equilibrium in the outflow. With the equilibrium CH_4
410 reached and the known pumping rate through the probes, it is then possible to calculate
411 emission rate (See Sect. S.4.3 in SI).
412
413 **2.4.4 Hole method, based on leak and pipeline properties**
414 The LDC reported the physical properties of gas leaks and pipeline conditions. These include
415 leak area, pipeline diameter and pipeline operational pressure. In order to get an estimate of the
416 upper physical limits of gas leakage through a hole with the given properties, we used the
417 empirical model by Liu et al., (2021), which was designed to quantify emissions from buried

418 natural gas pipelines to estimate emission rates from the leaks (Eq. 3), hereinafter "hole"
419 method.
420
421 $Q = 0.567 \cdot [(h + 139.592)^{-0.1} – 0.542] \cdot d^{1.5} \cdot p^{0.7}$ Eq. 3
422
423 Here, Q is the gas leak rate in $m^3\ h^{-1}$ (at standard atmospheric conditions and converted to
424 NTP), h is the depth of the buried pipeline in cm, d is the gas leak hole diameter in mm and p
425 is the pipeline overpressure in kPa. We used 150 cm as pipeline depth for all the locations in
426 Hamburg to estimate emission rate. We note that the model that we employed is for buried
427 pipelines not pipelines in open space, and emission estimates for the gas leak emission rate in
428 open space would be even higher (See Sect. 4.4 in SI). Ebrahimi-Moghadam et al. (2018)
429 showed that CH_4 emission from a pipeline hole area can be between 7 to 10 times higher in
430 open space relative to the subsurface conditions.
431

3 Results

433
434 **3.1 Leak Detection**
435 15 possible leak locations were detected by the mobile method in the initial surveys, (labeled
436 as HH001 – HH015). At 13 out of these 15 locations, leaks were confirmed by the LDC, HH007
437 and HH012 locations were not confirmed as gas leak locations. In addition, the LDC identified
438 5 other leak locations (labeled as HH100 – HH104) that had not yet been fixed (category B and
439 C). The overview of the measurements (detection and quantification) is provided in the SI (See
440 Sect. S.5 in SI). At some locations we also observed that vegetation was impacted negatively
441 by the presence of leaks in their vicinities, a known phenomenon as high levels of methane
442 cause harmful anoxic conditions for the plant roots (See Sect. S.6 in SI). At several locations
443 the outlet identification was straightforward, because we only observed one outlet, but at 5
444 locations we observed numerous outlets spread over a large area. Figure 2 shows the spread of
445 emission outlets at one of the locations (Fig. 2a), with correlations of CH_4 and C_2H_6 at the
446 "strongest" outlet (Fig 2b). Fig. 2c shows precise gas leak location practice of the LDC at one
447 of the other locations.
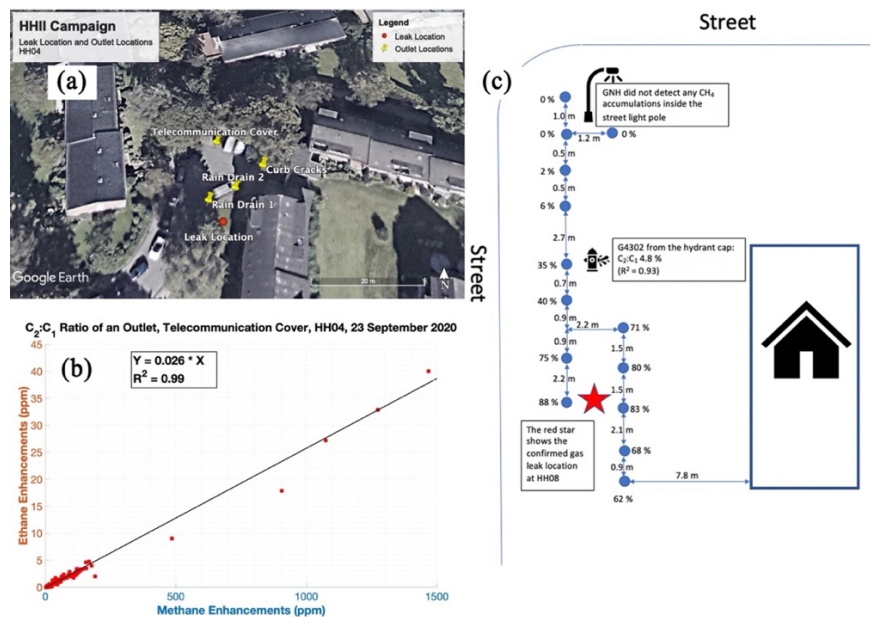
448
449 **Figure 2 – (a) aerial image of location HH004 (© Google Maps). Yellow pins show surface**
450 **emission outlet locations, and the red point shows the actual pipeline leak location**

451 **reported by the LDC; (b) correlation between CH$_4$ and C$_2$H$_6$ measured from a**
452 **telecommunication cover; (c) Map (not to scale) of drilled holes (blue dots) to locate the**
453 **pipeline gas leak at HH008. The red star shows the actual pipeline gas leak location as**
454 **indicated by the undersurface CH$_4$ mole fractions (See Sect. S.3, Fig. S3)**

455

456 **3.2 Leak Quantification**
457 Table 1 shows the results of the leak emission rate quantifications from the four methods. All
458 these locations were quantified by the mobile method, although for 6 of them the 10%
459 enhancement threshold was not reached. 16 locations were quantified by the tracer release
460 method and 8 by the suction method. A complete overview of key parameters for all
461 measurements (detection and quantification) is provided in Sect. S.5.

462

463 Table 1 – Results of gas leak quantification with different methods in Hamburg, Germany

	ID	Leak quantification methods (L min^{-1})							Info. from the LDC			
		Mobile (measurements from G2301)			Tracer (L min^{-1})	Suction		Hole (L min^{-1})	Pipeline buried year	Leak size (cm^2)	Leak type; Safety considerations	Pipeline Size and Material$^{\#}$
		Transect (s) w/ CH$_4$ Enh. > 10% threshold	Emission average	Emission range; 95% confidence		Emission (L min^{-1})	Status					
Detected by mobile method	HH001	n = 1 (10%)	0.7	-	0.06	<1.8	INC	39	1935	2.5	C	DN80ST
	HH002	n = 5 (50%)	4.9	0.7 – 36.0	0.22	<0.7	INC	45	1935	3.0	A2	DN80ST
	HH003	n = 6 (86%)	7.5	1.1 – 53.0	1.37	-	-	-	1963	-	A1	DN100ST
	HH004	n = 4 (100%)	7.8	1.8 – 34.5	5.33	-	-	-	1959	-	A1	DN80ST
	HH005^{+}	n = 19 (51%)	1.8	0.9 – 3.6	0.21	-	-	-	1935	-	A2	DN80ST
	HH006*	n = 11 (39%)	1.2	0.8 – 1.8	0.02	0.3	CPLT	33	1934	0.5	B	DN80ST
	HH007°	n = 0 (0%)	-	-	-	-	-	-	-	-	-	-
	HH008	n = 6 (26%)	1.5	0.4 – 6.4	0.32	<1.3	INC	-	1934	-	C	DN80ST
	HH009$^{\times}$	n = 9 (38%)	3.9	1.5 – 9.8	4.86	<3	INC	-	1928	-	A1	DN80ST
	HH010	n = 3 (38%)	1.6	0.2 – 13.7	0.51	<0.7	INC	-	1937	-	C	DN200ST
	HH011$^{\wedge\times}$	n = 4 (50%)	1.9	0.2 – 18.6	0.37	-		150	1963	15	A1	DN300ST
	HH012°	n = 0 (0%)	-	-	-	-	-	-	-	-	-	-
	HH013$^{\wedge}$	n = 2 (40%)	1.8	-	-	-		65	1939	5	A1	DN80ST
	HH014	n = 24 (55%)	1.6	1.1 – 2.5	1.41	-	-	65	1950	5	A1	DN100ST
	HH015	n = 1 (50%)	1.0	-	0.38	<0.9	INC	19	1935	1	A1	DN80ST
Reported by the LDC	HH100	n = 1 (13%)	0.7	-	0.14	-	-	-	1994	-	C	d225Pe
	HH101	n = 0 (0%)	-	-	0.07	<0.7	INC	-	1960	-	C	DN80ST
	HH102	n = 0 (0%)	-	-	0.01	-	-	-	1928	-	C	DN125ST
	HH103	n = 0 (0%)	-	-	0.03	-	-	-	1963	-	B	DN150ST
	HH104	n = 0 (0%)	-	-	-	-	-	-	1930	-	C	DN100ST

464 $^{+}$ The LDC reported three leak locations, ≈ 30 m distance between the two ends, for this
465 location: two leaks with area of 5 cm^2 and one leak with area of 1 cm^2
466 * Complete measurements for the suction method and used for averaging
467 ^ Leak size reported as sum of total hole area of all the leaks on the pipeline
468 $^{\times}$ Large difference between leak location and the tracer release location
469 $^{\circ}$ The LDC did not confirm a gas leak

Pipeline materials, steel (ST) or Polyethylene (Pe), pipeline Diameter Nominal (DN), which is close to the inner pipeline diameter in mm

3.2.1 Mobile method

The mobile method was applied at all the 20 locations (18 confirmed and 2 unconfirmed gas leak locations). At 14 (all confirmed gas leak locations) out of the 20 locations, CH_4 enhancements above the 10% threshold were observed and could be evaluated with the standard algorithm. The emission rate estimates for these 14 gas leak locations ranged from 0.7 to 7.8 L min^{-1}. At the 6 other locations we didn't observe any CH_4 enhancements above the 10% threshold. When we lowered the enhancement threshold to 10 ppb, the emission rates were 0.07 (HH007; not confirmed gas leak location), 0.1 (HH012; not confirmed gas leak location), 0.04 (HH101), 0.02 (HH102), 0.05 (HH103) and 0.02 L min^{-1} (HH104). Of the 5 leak locations reported by the LDC, 4 did not show any enhancement maximum above the 10% threshold, i.e., these locations would not have been identified with the default algorithm (Weller et al., 2018) and would thus not produce an emission estimate.

Fig. 2 shows a summary of all individual observed enhancement maxima with the G2301 analyzer from all transects with the mobile vehicle, which were used for the quantification of emission rates with Eq. 1. The figure illustrates the large spread in enhancement maxima for multiple passes at each location, similar to Luetschwager et al (2019), leading to large uncertainties in emission estimates of individual locations. Fig. 2 also shows the diversity of the various locations, where at some locations most or all of the observed enhancement maxima are above the 10% threshold (e.g. HH003 and HH004), at several locations none of the enhancement maxima was above the threshold (e.g. HH101 and HH104) and at other locations many transects showed enhancement maxima both above and below the threshold (e.g. HH006, HH008, HH009, HH014).

As shown in Fig. 3, there is a wide range of CH_4 enhancement observations per location. This depends on wind conditions, distance of the observed plume maximum to the emission outlet location, the superposition of emissions from several outlets and likely other variables such as soil water content. The mean relative uncertainty from the mean emission rate values for the mobile method is ≈ 70% for lower and 400% fort the upper ends for the locations with at least 3 transects (n = 10) which pass the 10% enhancement threshold (significant signals) in this study. The lower and upper ranges go down to 60% and 275% for the locations with at least 5 transects (n = 7) with significant CH_4 enhancements.
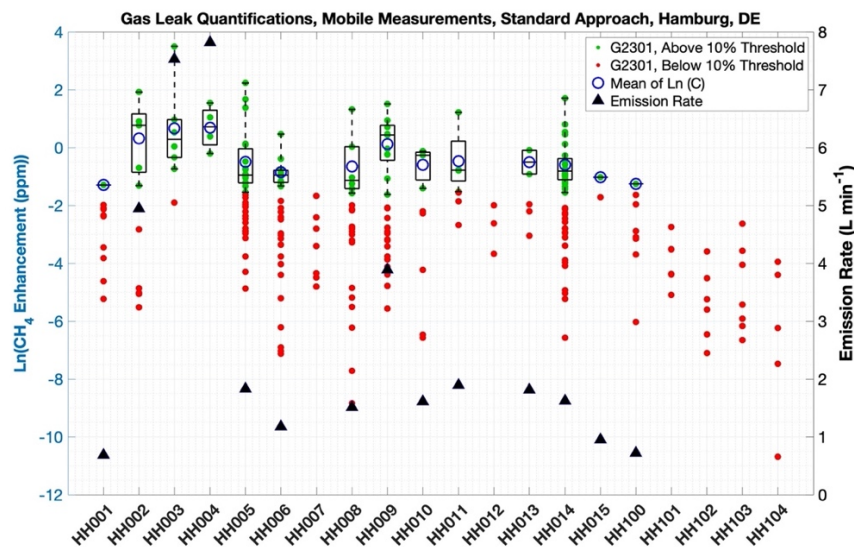
Figure 3 – CH_4 enhancement maxima from all individual transects for each location using G2301. Red points show CH_4 enhancement maxima below the 10% threshold, green

points show CH$_4$ enhancement maxima above the 10% threshold, thus used for the standard quantification. Blue circles show the $\overline{\text{Ln} \, (C_{max})}$ of all the green points for each location, and black triangles show the derived mean emission rate (based on all green points) using Eq. 1 for the location with at least one green point (right y-axis).

3.2.2 Tracer method

The tracer method performed emission rate quantification at 16 gas locations out of 20 locations. The derived emission rates range from 0.03 to 5.3 L min^{-1} (Table 1). For 4 locations the tracer method was not applied because (i) the emissions were not persistently observable and the LDC also didn't confirm existence of gas leaks at these locations (n = 2; HH007 and HH012) or (ii) the leak had already been repaired (n = 1; HH013) or (iii) no emission was detectable during the visit of the tracer team (n = 1; HH104). For two of the locations (HH11 and HH09), where leaks were confirmed and the tracer method was successfully deployed, later investigations during repair actions (see Fig. 1) showed that the surface emission outlets were located far (15 to 60 m) from the actual gas pipeline leak location indicating underground gas migration. It is evident from Table 2 that the tracer technique can also quantify very small emission rates, below the cut-off of the mobile technique of 0.5 L min^{-1}. Emission rate estimates derived from the tracer technique were in general lower than the ones derived from the mobile technique, except for three sites where those were comparable (HH004, HH009 and H014).

3.2.3 Suction method

Due to the time-consuming nature of the suction measurements, initially 10 gas leak locations had been planned for deployment of the suction method in this campaign. The goal was to cover a wide range of expected emission rates, as stated in the intercomparison matrix. The suction method was applied at 8 gas leak locations (see Table 1). At only one location the quantification could be completed according to protocol where an equilibrium mixing ratio has to be reached. This was at HH006, with a derived emission rate of 0.3 L min^{-1}. At several of the locations where the mobile method had indicated high emission rates, subsurface accumulation was widespread, and the suction method was either not deployed (n = 3; HH003, HH04, HH011) or the measurements were incomplete (n = 7; HH001, HH002, HH008, HH009, HH010, HH015 and HH101) because of either safety reasons or because the suction team estimated that they would be unable to complete the measurements within a day. For the 7 locations with incomplete suction measurements, the emission rates were reported ranging from 0.7 to 3 L min^{-1}. These can be regarded as upper limit estimates because suction was not yet completed and CH$_4$ mixing ratios would have likely dropped further.

3.2.4 Hole method

For 5 locations where the leak area of a single gas pipeline leak was reported, the corresponding emission rates are between 19 to 65 L min^{-1}. For locations HH011 and HH013, the hole area was reported as the sum of several holes and the total hole area for these two locations resulted in an emission rate of 150 and 65 L min^{-1}, respectively. The quantification from the hole method is higher than from the mobile, tracer and suction methods by at least an order of magnitude.

3.3 Leak categories

The 20 (18 confirmed + 2 not confirmed) locations can be divided into four main categories related to measurement challenges of the various methods. These categories may overlap.

      (i)   Large subsurface CH$_4$ accumulation
      (ii)   Insufficient CH$_4$ enhancements for mobile quantification
      (iii)   Large CH$_4$ enhancement variability for mobile quantification

556   (iv)   Several outlets and / or leaks or atmospheric turbulence

557 In this section we present the overall results and discuss in detail one selected location for each
558 of these categories. The remaining locations (with similar characteristics) are presented in the
559 SI.

560

561 3.3.1 Location type I – Large subsurface CH_4 accumulation and multiple outlets

562 The spatial spread of surface emission outlet locations identified with the G4302 instrument as
563 part of the mobile method provides an indicator for the extent of the subsurface accumulation
564 of CH_4. For 5 locations, emission outlets were found at great distance from each other, in order
565 of tens of meters. The total emission of a gas leak is equal to the sum of emissions from all the
566 surface outlets at a location, thus it is necessary to quantify each outlet separately to get the
567 total emission.

568 HH011 (Fig. 4) is an example where very widespread CH_4 accumulation and migration was
569 observed. During the initial mobile gas leak detection, leaks were located at the intersection of
570 streets 1 and 2, close to a subsurface vent and a rain drain, $\approx$ 2 m apart, (the yellow pin in Fig.
571 4a) based on clear signals from these outlets and a sign next to the road indicating presence of
572 gas pipelines. The vent showed a $C_2:C_1$ ratio of 2% (R^2 of 0.8 and max CH_4 mole fraction of
573 31 ppm) and we observed $C_2:C_1$ ratio of 2.8% with R^2 of 0.96 and max CH_4 mole fraction of $\approx$
574 70 ppm from the rain drain, clearly indicating a large / dominant contribution from fossil CH_4.
575 However, after quantifying the emission from these two leaks using the mobile and the tracer
576 release methods, the LDC found the actual gas pipeline leak, during the repair actions, on the
577 south side of the intersection, far from the vent and the rain drain, at the intersection of street
578 no. 3 and no. 2 indicating that the gas had travelled about 60 m underground. It is possible that
579 the leak resulted in several gas emission outlets, likely closer to the gas pipeline leak location.
580 The emission rate measured using the mobile method was 1.6 L min^{-1} based on 5 plume
581 transects and is likely underestimated because some emission outlets potentially were not
582 included in the performed plume transect. It should also be noted that the distance from the gas
583 pipeline leak location to the plume transect is larger than the distances applied during the
584 controlled release calibrations (average 15 m) (Weller et al., 2019).

585 The tracer was released at the vent and the rain drain and thus measured the combined emission
586 from these two outlets to be 0.4 L min^{-1}. If the gas pipeline leak gave rise to multiple
587 unidentified surface emission outlets, the emission from the gas pipeline is underestimated. IN
588 fact, Fig. 4b shows that a CH_4 plume without C_2H_2 was observed during the tracer release
589 measurements at HH011, confirming that at least one other source of methane emission was
590 present nearby.

591 Based on the previous experience at locations with widespread subsurface accumulation it was
592 concluded that the suction method could not be applied at this location. The other case in this
593 category was HH009.
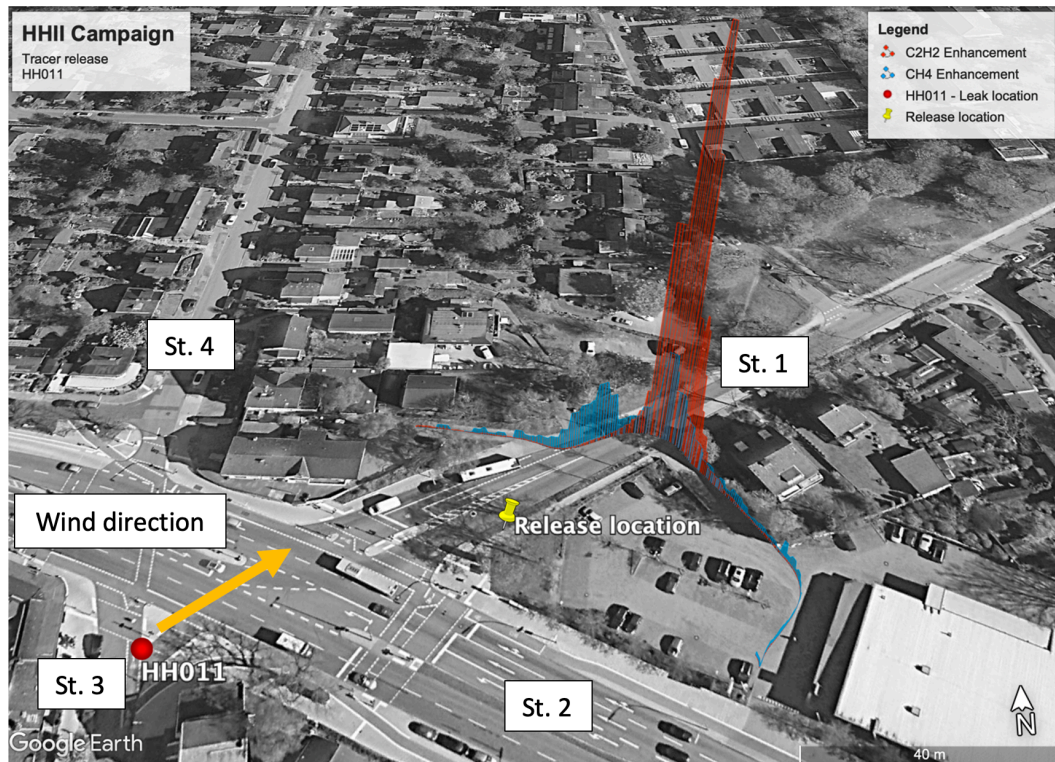
594
595 **Figure 4 – aerial image of HH011 (© Google Maps). A gas leak location with widespread**
596 **undersurface CH$_4$ accumulation. The yellow pin shows the assumed leak location and**
597 **location of tracer release, which was very different from the actual leak location as**
598 **identified by the LDC (red circle). St. 1-4 are added to identify streets that are discussed**
599 **in the text. General wind direction during tracer release deployment is shown with an**
600 **orange arrow. CH$_4$ (in blue) and C$_2$H$_2$ (in red) levels measured at a plume transect. One**
601 **of the CH$_4$ plume is proportional to the C$_2$H$_2$ plume while the other CH$_4$ plume lacks the**
602 **C$_2$H$_2$ signals suggesting existence of at least another emission outlet.**

603
604 The LDC reported the total area of several holes in the pipeline as 15 cm^2 for HH011, which is
605 the largest leak size among all the locations. If we assume that there was one hole with this
606 size, then the emission rate estimated by Eq. 3 will be 150 L min^{-1}, a hole of 5 cm^2 gives
607 emission rate of 65 L min^{-1}. The pipeline for this location was DN300ST and has been in
608 operation since 1963.

609
610 **3.3.2 Location type II – Insufficient CH$_4$ enhancements for mobile quantification**
611 At HH101, on a narrow (≈ 3 m wide) street, which had about 1 m wide bare soil pavement on
612 one side, the LDC reported a gas leak location based on their routine surveys. On both sides of
613 the street there were about ≈ 1.5 m tall bushes and some trees. All three methods (mobile, tracer
614 and suction method) were deployed at this location. Gas emissions found their way to the
615 atmosphere through cracks in the asphalt with C$_2$:C$_1$ ratio of 2.5% (R^2 of 0.93) with max CH$_4$
616 mole fraction of ≈ 25 ppm. None of the CH$_4$ enhancement maxima observed during the mobile
617 surveys at this location were above the 10% enhancement threshold with the G2301 instrument,
618 thus this location would not be labeled as LI and no quantification would be reported from
619 mobile method as implemented in Weller et al (2019) and Maazallahi et al. (2020). The tracer
620 method was applied in static mode at a distance of ≈ 15 m and reported an emission rate of 0.1
621 L min^{-1}, which is compatible with the emission strength being below the "detection limit"
622 defined by the 10% cut-off of the standard algorithm (0.5 L min^{-1}). When the emission strength
623 is evaluated using the CH$_4$ enhancements below the cut-off, the value is 0.04 L min^{-1}. The

624 suction method was applied at this location but an equilibrium was not achieved after 9 hr, i.e.
625 incomplete suction measurements, and an upper limit for the emission rate of ≈ 0.7 L min^{-1} was
626 reported. The fact that the suction measurement was incomplete at this location with a small
627 emission rate shows that subsurface accumulation can also be large for smaller leaks.
628 Three of the leak locations in this study only showed one CH$_4$ enhancement above threshold.
629 The 10% threshold is a constraint, which removes enhancements less than about 200 ppb. This
630 means for the locations where we only have one transect with CH$_4$ enhancements more than
631 the 10% threshold, the minimum emission rate estimated is about 0.5 L min^{-1}, no matter how
632 many transects we had with CH$_4$ enhancements less than the 10% threshold. This situation was
633 observed for HH001, HH015 and HH100 (Fig. 5). In this case, the mobile method likely
634 overestimates the total leak rate, because only the maximum enhancement is used for
635 quantification. The tracer method reported low emission rates for these three sites 0.12 L min^{-1}
636 ^{1} on average (n = 6).
637 For the two locations (HH007 and HH012) where the LDC didn't confirm gas leaks (despite
638 periodic observation of C$_2$H$_6$ at outlets during the mobile surveys) none of the transects showed
639 CH$_4$ enhancement maxima above the 10% threshold. At HH007, the outlet was through cracks
640 in the pavement but at HH012 the outlets were from manholes. At HH007 the outlet location
641 had shifted by about 2 m for two different days (4-week gap). We note that the correlation
642 coefficients between CH$_4$ and C$_2$H$_6$ at these locations were between 0.4 and 0.6, so less than
643 0.7, which is the threshold correlation we accepted for the outlets. As a leak was not confirmed
644 for these locations, the tracer and suction methods were not applied.
645
646 **3.3.3 Location type III – Large CH$_4$ enhancement variability for mobile quantification**
647 For several locations, we observed a large variability of CH$_4$ enhancements from different
648 transects. One example is HH008, where only 6 of the 23 transects exceeded the 10% threshold,
649 i.e. the leak was only observed in about every 4th transect. The leak location of HH008 is an
650 example where CH$_4$ enhancements from several transects cover a wide range. Based on the 6
651 transects, which showed enhancement maxima above the 10% threshold, a leak rate of 1.5 L
652 min^{-1} is derived. This may be an overestimate since many transects with maxima below the
653 threshold were not considered. For this location the mobile tracer method was applied, which
654 resulted in a leak rate quantification of 0.3 L min^{-1}.
655 The suction method derived an upper emission estimate of 1.3 L min^{-1} from incomplete
656 measurements at HH008. The LDC reported a C category leak for this location from a DN80ST
657 pipeline, which was installed in 1934.
658
659 **3.3.4 Location type IV – Several outlets and / or leaks or atmospheric turbulence**
660 On a ≈ 5 m wide street, we detected two leaks about 80 m away from each other, HH001 and
661 HH002 (Fig. 5a). It was a cobblestone street and there were bushes and few trees planted,
662 mostly on one side of the street. The mobile method performed 10 transects at both locations
663 and all the transects were accepted for the evaluation. The tracer team could quantify both
664 locations using static measurements. The suction team began to quantify HH002 and HH001,
665 but during quantification of HH001, there was a small accident (fire due to contact of drilling
666 head with electric cable) and the leak had to be fixed immediately. The plumes on this street
667 were sufficiently separated to positively identify two different leaks on the same street. In
668 contrast, at location HH005, we observed several maxima for the same transect, but because
669 the maxima were close to each other, those were clustered together in the mobile measurement
670 algorithm (Fig. 5b). Later the LDC reported even three individual pipeline leaks on this street.
671 In another example (HH010), some transects showed several plume maxima although only one
672 emission outlet and later on only one gas pipeline leak was found (Fig. 5c). However, the
673 release of the tracer resulted in several matching CH$_4$ and tracer gas plumes confirming that

674 the emission indeed occurred form a single outlet and that the multiple plumes at this location
675 were due to inhomogeneous plume dispersion. This illustrates that the existence of several
676 maxima in one transect does not necessary correspond to presence of several leaks and/or
677 outlets, but it can also be related to a spatially heterogeneous/disturbed plume. This shows that
678 the signals from the mobile detection method are not sufficient to allow determining the
679 number of leaks at a location with several plume at a close distance from each other in a single
680 transect.
681
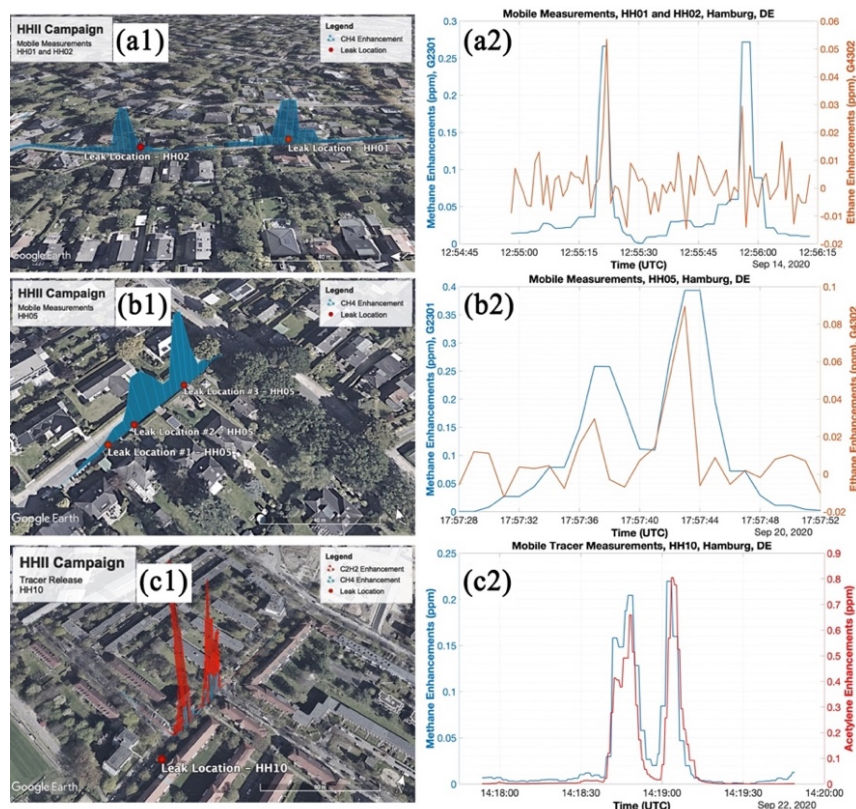
682
683 Figure 5 - Several maxima observed during a single transect on one street showing
684 different situations: two well isolated leaks with about 80 m distance from each other (a1
685 and a2, HH001 and HH002), three pipeline leaks close to each other with several emission
686 outlets (b1 and b2, HH005) and one leak and one outlet but several CH₄ enhancement
687 maxima due to turbulence (c1 and c2, HH010), aerial images: © Google Maps.
688
689 After detection by mobile measurements, emissions out of the ground were detected at HH001
690 and HH002 with the G4302 backpack within 3 m distance from the gas pipeline leak locations,
691 which was later reported by the LDC. For the single transect with a maximum above the 10%
692 threshold observed with the mobile method, the derived emission rate at HH001 was 0.8 L min⁻
693 ¹ (n = 1). For HH002, the derived emission estimate for the transects with maxima above the
694 threshold is 5.2 L min⁻¹ (n = 5) from the mobile method. At HH002, individual derivation of
695 emission from separate CH₄ enhancement gives a wide range between 0.7 and 36.0 L min⁻¹
696 (95% confidence) from the mobile method (see category III above). For HH001, the tracer
697 method was applied in static mode at ≈ 30 m distance to the release point and ≈ 40 m far from
698 HH002. The derived emission rate for HH001 is 0.06 L min⁻¹ and for HH002 0.22 L min⁻¹ from
699 the tracer method. For HH001, after about 5 hr of pumping, the suction quantification had to
700 be stopped due to the incident described above. Based on the incomplete suction measurement
701 an upper limit for emission rate of ≈ 1.8 L min⁻¹ for HH01 was estimated. An emission estimate
702 of ≈ 0.7 L min⁻¹ was derived for HH002 from an incomplete suction measurement. The LDC

703 reported leak size of ≈ 2.5 cm² for HH001 and for ≈ 3 cm² for HH002 which then give emission
704 rate of 39 and 45 L min⁻¹ respectively from the hole method. For both locations, leaks were due
705 to pipeline corrosion.
706
707 **3.4 Emission rates of different leak safety types**
708 The 18 confirmed gas leak locations that were investigated in the campaign were categorized
709 into the four safety categories, A1 (n = 7), A2 (n = 2), B (n = 2) and C (n = 7). The mobile
710 method quantified all the A1 and A2 leaks (n = 9) with an average emission rate of 3.6 L min⁻¹
711 ¹. 5 out of 9 leaks in categories of B and C leaks were quantified with the mobile technique
712 including the 10% threshold with average emission rate of 1.1 L min⁻¹ (n = 5). Apart from one
713 location, which had to be fixed before the measurements, the tracer method quantified the A1
714 and A2 leaks (n = 8) and reported an average emission rate of 1.8 L min⁻¹. The tracer method
715 also quantified all the B and C leaks (n = 9) with an average emission rate of 0.1 L min⁻¹.
716 Mostly due to the safety and time constraints and medium to large underground accumulations
717 of CH_4, the suction method could provide incomplete measurements at only 3 locations of A1
718 and A2 leaks with an average emission rate of 1.5 L min⁻¹ (n = 3). The suction method measured
719 at 5 out of 9 B and C locations, one of the measurements was complete and the others were
720 incomplete, with an average emission rate of 1.0 L min⁻¹ (n = 5). Although the number of
721 quantified leaks is limited, all the three methods show that the emission rates from category A1
722 and A2 leaks are higher than category B and C leaks (Fig. 6). This indicates that the site
723 selection bias of measurements for the suction method due to safety concerns (see qualifier
724 above), can lead to a bias in the emission rate in this method. Except for three leaks (HH003,
725 HH009 and HH011), leaks were located by the repair team where the carpet method reported.
726 These three leaks were finally found at some distance from the location initially indicated by
727 the carpet method. These three leaks are medium or high emitters and belong to type A1.
728 Although the number of locations in this study is very small, this supports the common sense
729 assumption that bigger leaks can spread out more widely in soil and contaminate larger
730 undersurface area. Therefore, the bigger leaks may be mislocated by the carpet method, and
731 they are also more likely to fill cavities, placing them in a higher safety category.
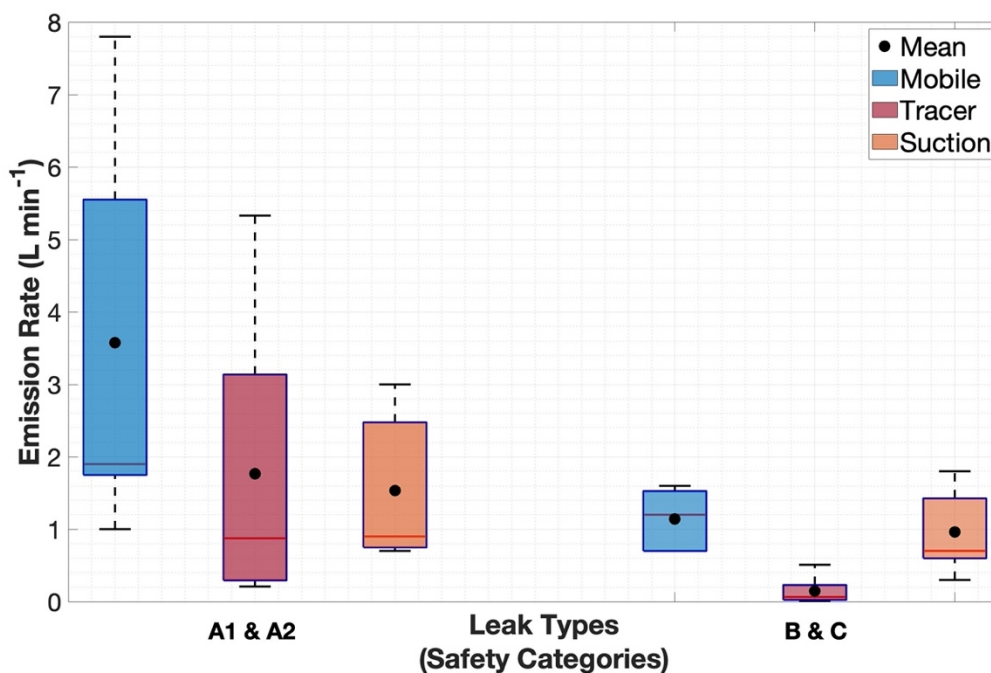
732
733 **Figure 6 – Emission rate differences between different gas leak safety categories.**

4 Discussion

4.1 Leak detection methods

4.1.1 Leak location vs outlet location

There is a difference between the location of the leak in the gas pipeline (leak location; See Sect. S.7 in SI) and the location where the gas is emitted to the atmosphere (outlet locations; See Sect. S.2 in SI). Furthermore, a single leak in the gas pipeline can result in multiple emission outlets at the surface. In this campaign we observed that in most cases (2 out of 18), the emission outlet at the surface occurred only a few m (sometimes < 1 m) from the location of the leak in the gas pipeline. However, in one case, an emission outlet was detected about 60 m away from the leak location indicating significant underground gas accumulation and migration (see Fig. 4).

4.1.2 Intercomparison of the gas leak detection methods

The mobile method detects atmospheric CH_4 enhancements while measuring continuously with ppb precision from an inlet installed at the front bumper of the car while LDCs apply the carpet method with an instrument precision at the ppm level. High precision for the carpet method is not needed as the inlet to their instruments is connected to a carpet, which is attached to the ground. The mobile method can cover larger areas in shorter times, but not all roads, walkways, or other surface areas where pipelines are buried are accessible with a vehicle. The advantage of the carpet method is that it can precisely follow the pipeline map, which also means that it can locate leaks more precisely. The mobile method uses a 10% threshold to neglect unreliable gas leak sources, which sometimes results in neglecting actual signals from small leaks. Also the mobile measurements do not detect all leaks due to the dependence on the wind direction (only downwind sources leaks can be detected). Luetschwager et al. (2021) suggested that 5 to 8 plume transects give > 90% probability of gas leak detection at a given location, so if all the streets in an urban area are covered 5 to 8 times, > 90% of the leaks can be detected by mobile measurements.

Both the mobile and the carpet method use C_2H_6 signals for distinguishing between fossil and microbial CH_4 emissions, and as for C_2H_6, the instrument used in the mobile method is more sensitive, and faster. In the carpet method, the laboratory analysis of C_2H_6 is slow and with higher detection threshold compared to the mobile method, where C_2H_6 is measured in real-time during the surveys, and also on foot from the emission outlet. The CRDS instrument provides real-time measurements of CH_4 and C_2H_6 at 1 Hz frequency so checking various outlets at a possible gas leak location is faster.

At 14 out of the 20 locations in this study, gas leaks were detected (CH_4 signals passing the 10% threshold) and quantified with the mobile method. However, we observed that 4 out of 5 locations reported by the LDC would not have been detected in mobile surveys without prior information on existence of the leaks because the maximum enhancement was below the mobile detection threshold. At the only location (HH100) from the list of the LDC, where mobile method could quantify the emissions, the outlets were located on the road and the vehicle was driving on top of the outlet. For this location only one of the transects passed the 10% enhancement threshold, and the quantification for this location was ≈ 0.7 L min^{-1}, close to the detection threshold of this method, ≈ 0.5 L min^{-1}. One of the other locations, HH101, reported by the LDC had similar surrounding conditions (e.g. presence of buildings, road conditions, etc.) as the other leaks detected by the mobile method, but still the mobile method was not able to detect a gas leak at this location without a priori information from the utility. The quantifications made by the tracer method suggest that the emission rates of the locations provided by the LDC were much lower than the locations detected by mobile measurements

782   (Table 1). The 10% threshold in the mobile method precludes the identification of small leaks
783   (< 0.5 L min^{-1}), which would only be identified by the carpet method.
784
785   **4.2   Signal attribution in mobile detection method**
786   **4.2.1 Attribution during mobile survey in car**
787   During the mobile measurements we used two approaches to find correlation between CH_4 and
788   C_2H_6. When we compare the online measurements point by point, the probability of detecting
789   a fossil signal is high, as only one single significant reading is sufficient to indicate a fossil
790   signal. When we use the R^2 of the linear correlation between CH_4 and C_2H_6 enhancements
791   above the cut-off, the attribution is more reliable. In a large dataset without a priori information
792   on the existence of a gas leak at different locations, the correlation method is more trustworthy
793   as the point-by-point method could be affected by instrument noise and/or spikes.
794   We also used CO_2 signals and their correlation with CH_4 signals to investigate interference
795   from combustion or microbial processes. For only 7 plumes at 6 locations, we detected
796   correlations between CO_2 and CH_4, which could indicate either oxidation of CH_4 to CO_2 or
797   mixture of microbial CH_4 emissions from e.g. the sewer system with the emissions from natural
798   gas leaks. The number of these possible co-emissions is low compared to the number of total
799   transects (only $\approx$ 7% of the plumes with CH_4 enhancements greater than 10%), thus such an
800   admixture of microbial CH_4 should not impact the quantification from mobile method
801   significantly.
802
803   **4.2.2 Plume attribution to emission outlets**
804   The outlet attribution was performed using the G4302 CRDS instrument which is portable like
805   a backpack. We checked the outlets (See Sect. S.2, Fig. S1) around the locations of interest and
806   evaluated the correlation between CH_4 and C_2H_6 and the persistence of the emissions on
807   different days. In theory, it is possible to estimate contributions of fossil and microbial CH_4 in
808   a plume using the ethane signals during the mobile measurements with the vehicle and the
809   reference C_2:C_1 ratio provided by the LDC. However, due to the low C_2H_6 signals in ambient
810   air, it was not feasible to quantify the possible contribution of microbial methane emissions.
811   Nevertheless, the C_2H_6 signals of the G4302 CRDS instrument were still very useful to identify
812   a location as a possible gas leak location or not. For all the 15 locations, which were initially
813   detected by the mobile method we observed detectable C_2H_6 signals, including the two
814   locations which later were not confirmed as a gas leak location by the LDC. This suggests that
815   either the leak is at a greater distance and depending on the transport of the emission we
816   periodically can see the signals at the detected outlets or that there are sources that produce
817   both CH_4 and C_2H_6 in the vicinity of the location.
818
819   **4.3   Leak quantification methods**
820   **4.3.1 Mobile method**
821   If the outlets are close to each other, we may observe several CH_4 enhancements close to each
822   other or overlapping when a single transect is performed at a close distance. If we assume that
823   the number of CH_4 maxima is equivalent to the number of real outlets that exist on a road and
824   only use the maximum enhancements from the most pronounced plume to calculate the
825   emission rate, the total emission will be underestimated with the mobile method.
826   Emission rate estimates with the mobile method from individual transects are associated with
827   high uncertainty, related to variabilities in either above-ground or under-ground conditions. For
828   example, an unfavorable wind direction (above ground condition) can result in missing a plume
829   from a gas leak. The mobile measurement van itself may also affect the measurement, e.g., by
830   creating pressure fluctuations. Luetschwager et al. (2021) showed that the quantifications from
831   the same leak in individual mobile transects can vary by more than an order of magnitude. In

832   Hamburg, we found that the range can be even a factor 50 or 100 in exceptional cases (Table
833   2). This high variability illustrates that if we perform only one transect per location, the
834   estimated leak emission rate can result in high under / overestimation in emission estimate for
835   the single location, as was also reported by Maazallahi et al. (2020). This large uncertainty for
836   individual locations is less severe when the results are extrapolated to the city-level, where the
837   sample size is also large, including over- and underestimates (Brandt et al., 2016).
838   In our previous study in Hamburg (Maazallahi et al., 2020) the overall average emission rate
839   for all the LIs was estimated 3.4 L min^{-1} LI^{-1} (n = 145) while for the fossil-attributed
840   locations it was 5.2 L min^{-1} LI^{-1} (n = 45; standard error of 3.1). This showed that the biggest
841   emitters were among the fossil categories. In the present study, the average emission rate from
842   mobile measurements for the gas leak locations is 2.7 L min^{-1} LI^{-1} (n = 14; standard error of
843   0.6). The higher average emission rate per fossil location in the first campaign may have been
844   caused by the fact that in that campaign only a smaller number of transects were performed per
845   location (on average 1.1 in the precious study versus 6.9 transects with CH_4 > 10% threshold
846   per location in the present study). Luetschwager et al. (2021) stated that after 6 transects with
847   CH_4 exceeding the 10% threshold per location the average overestimation of leak size estimates
848   will be less than 10%. In addition, the differences in sample size and locations in these two
849   studies (45 versus 14 locations in the first and second studies respectively) may partially
850   explain the difference in average. This is because the probability of detecting large emitters,
851   which increase the average emission rate of all leaks, increases with sample size.
852   The two CH_4 sensors onboard the mobile van play specific roles in the detection and
853   quantification of leaks. CH_4 enhancements on the G2301 are 3.8 times lower than the G4302.
854   This is an artefact of the G2301, which smoothes the signal compared to the G4302 because of
855   the slower pump and sampling rate (See Sect. S.8.1 in SI). On the other hand, this results in
856   more signals passing the 10% threshold on G4302. This then also leads to higher detection
857   probabilities using G4302 (See Sect. S.8.2 in SI). Higher record of CH_4 enhancements also
858   results in higher emission rate quantification using Eq. 1 (See Sect. S.8.3 in SI). We use the
859   G2301 for quantification, since this is the instrument that was also used for introduction of the
860   mobile equation quantification in Weller et al. (2017). The quantification of the gas leak
861   locations using Eq. 1 depends only on the CH_4 enhancements. This gives about a factor 2 higher
862   emission rates from G4302 than from G2301 for the same plumes. When we evaluate the plume
863   areas from the two instruments, they are much closer to the 1:1 line (See Sect. S.8.3 in SI). This
864   agrees with findings from another study using two different in-situ instruments onboard a
865   mobile car (See Sect. S1.5, Fig. S6 from Ars et al. (2020)). They also found that the plume area
866   is closer to the 1:1 line in mobile measurements even if the air intakes are not at the same
867   location of the vehicle. This suggests that the plume area is a more robust parameter than
868   maximum enhancement for emission rate quantification and a leak rate quantification equation
869   using the plume area should be developed.
870   In general, the closer the air intake is to the emission point the higher the CH_4 mole fraction
871   reading is (See Sect. S.9 in SI), but when several outlets are present at one location it is not
872   possible to uniquely determine the distance to the emission point, and also determine which
873   plume belongs to which outlet. Eq. 1 from Weller et al. (2019) only uses the maximum CH_4
874   enhancements above the 10% threshold from each pass. In their controlled release experiments
875   the average distance between the leak and measurement was 15.75 m. Analysis of our results
876   (Table S4, Sect S.5 in SI) shows that higher maximum mixing ratios are encountered more
877   often when the distances of the transect to the leak location are small. For example, at HH002
878   the transect was very close to the main emission point, which likely leads to the substantially
879   higher emission rate estimate derived from the mobile method (4.9 L min^{-1}) compared to the
880   tracer method (0.22 L min^{-1}). On the other hand, at HH011 the mobile method underestimates
881   the emission rate (See Sect. 3.3.1), as at this location the measurement distance to the leak was

882 larger than reference distance of 15.75 m applied by Weller et al. (2019). This suggests that to
883 reduce the quantification error for individual leak locations, distance should also be included
884 in an improved transfer equation. Although distance is a parameter in some quantification
885 methods, e.g. gaussian plume dispersion, and not in others, e.g. in mass balance, to the best of
886 our knowledge, this is the first study providing field evidence that distance is a factor that can
887 affect emission quantification using the Weller et al. (2019) method.
888 The effect of neglecting or retaining the transects with enhancement maxima below the 10%
889 threshold was quantitatively investigated for 5 locations where the tracer team conducted
890 mobile measurements (See Sect. S.10 in SI). These measurements were evaluated as
891 "controlled release" experiments for C_2H_2, because the actual C_2H_2 release rate is known, and
892 measurements were made in mobile mode. The standard mobile quantification algorithm with
893 the 10% threshold yields emission estimates that are in relatively good agreement with the
894 released quantities, whereas the estimates are biased considerably low when measurements
895 with maxima below the threshold are retained. This supports the use of the original method,
896 which removes transects with an improper realization of the plume. Relating to section 4.5, it
897 must be noted, however that in these measurements the distances of the C_2H_2 maxima to the
898 release points were between 30 to 45 m, thus larger than the normal distance of mobile CH_4
899 measurement to the emission outlets (from few meters up to 30 m).
900
901 **4.3.2 Tracer method**
902 The tracer method is more labor intensive than the mobile method. However, the strength of
903 the method is the application of a tracer gas providing the plume dilution and avoiding the use
904 of atmospheric dispersion models and weather information. If the tracer release location does
905 not reflect the sum of all the outlet emissions at a gas leak location, or misses some of the
906 outlets, then the total emission quantification from the gas leaks will be underestimated. An
907 example of such a case is site HH011 in this study where the leak location in the gas pipeline
908 (after quantification; see Fig. 1) was found to be located about 60 m upwind the targeted
909 emission outlet. During tracer quantification, an additional CH_4 plume (not defined by the
910 tracer gas) was observed indicating more than one emission outlet (Fig. 4). The confirmation
911 for this is the finding of gas leak location by the carpet method. The emission rate of the
912 targeted emission source (the vent and the drain) is thus not representing the combined
913 emission from the gas leak in the pipeline located 60 m upwind the emission source. Further
914 surface screening and leak detection would have been needed to identify and quantify all
915 emission outlets.
916
917 **4.3.3 Suction method**
918 The suction method is the most labor-intensive quantification method. Following a strict, safety
919 first, protocol the gas utilities fix leaks in the A1 safety category immediately upon detection
920 and A2 leaks within a week. Given logistical constraints, the suction method therefore mainly
921 or exclusively quantifies B or C leaks (50% of confirmed gas leak location in this study). We
922 investigated whether such a site selection bias could lead to a bias in the average quantified
923 emission rate in the inventory report. In this study, we observed that the leaks detected from
924 the mobile methods were mostly in the A1 and A2 category and the biggest emitters (based on
925 the mobile and tracer release measurements) had soil CH_4 accumulation of a magnitude that
926 prevented successful application of the suction method. Further research is needed to identify
927 the physical mechanism(s) to explain the observed correlation between A1 and A2 leaks and
928 high emission rates. As a hypothesis, the presence of soil cavities associated with leak category
929 A1 may result in higher permeability, i.e. lower underground resistance, which then leads to
930 higher emission rate for the same pipeline hole size compared to locations with no cavity.

The suction method was intended to be deployed right before the repair actions. For some of these locations, the suction method was in operation for more than 10 hours, but due to the high soil CH_4 accumulation, the measurements were stopped and labeled as incomplete in this study. For the other locations with high soil CH_4 accumulation, the suction method was not attempted, given the expectation (based on experience at the incomplete locations) that completion of measurements for leak rate quantification at those locations was unlikely.

4.3.4 Hole method

Based on the leak size, pipeline depth and overpressure, the average emission rate was estimated at 40 L min^{-1} (n = 5). We note that these estimated should be regarded as upper limits since flow restrictions outside the pipe are not included. The emission range of individual gas leaks based on the hole method is between 19 to 150 L min^{-1} for 1 cm^2 to 15 cm^2 hole sizes respectively, larger than any of the measurement-based quantification methods. This method requires information about the overpressure of the gas pipeline, depth of buried pipeline and size of a leak and it does not include the information about soil properties, which can impact the emission rate.

4.3.5 Intercomparison of methods

In this study, a reliable quantitative intercomparison of the three methods (mobile, tracer and suction methods) was attempted. A complete comparison of all three methods was possible at only one out of 20 locations (18 confirmed gas leak locations) because of the long time (>8-10 hrs) needed for full equilibrium of the suction method, whereby emission rates for 7 out of the 8 leaks quantified by the suction method were reported as maxima rather than absolute values (Table 1). At these 7 locations the emission was thus overestimated.

In total, the average CH_4 emissions from natural gas pipeline leaks for the same locations where we have quantifications from mobile and tracer methods (n = 13) are 2.8 and 1.2 L min^{-1} respectively. The suction method could only be completed at one location. The average emission rate reported for all the locations from the suction method (high bias due to incomplete measurement) is 1.2 L min^{-1} (n = 8).

The higher emission rates derived with the mobile method are in qualitative agreement with previous studies. Weller et al. (2018) compared quantifications from the mobile measurements described in von Fischer et al. (2017) with the tracer method and surface enclosure method in four US cities. They reported that mobile measurement estimates were $\approx$ 2.3 L min^{-1} greater than the tracer method mean estimates of $\approx$ 3.2 L min^{-1} (n = 59). This was attributed to the overestimation of small leaks (< 2.4 L min^{-1}) in the mobile measurements method, which we have also discussed above for our dataset. In addition, performance of only a few transects at individual locations also lead to systematically high biased emission rate estimates for higher emission rates (Luetschwager et al., 2021). Indeed, at the locations where we only have one transects with CH_4 enhancements above the 10% threshold, there is an overestimation from mobile method compared to the tracer method. For example, at HH001 (n=1), HH015 (n=1) and HH100 (n=1) the mobile method estimated emissions of a factor 4 higher in comparison to the tracer method. The analysis of Luetschwager (2019) clearly shows that this high bias is reduced when numerous transects are performed. Therefore, we carried out multiple transects to reduce this systematic bias. We note that there are also large differences between the mobile and tracer methods, e.g. HH002 and HH006. We suspect that the very short gas leak location distance to the mobile driving transects can explain partially the difference. Moreover, existence of another leak in the category of A1 at the HH006 location which had to be fixed prior to the tracer method could explain the difference in emission rate magnitude at this location. Nevertheless, the limited number of transects and the 10% threshold can contribute to an overestimation of the average leak rate with the mobile method at an individual location.

981 At the same time, however, the mobile method fails to detect leaks entirely when the leak outlet
982 is located downwind of the mobile van. The fact that the mobile method misses downwind
983 emissions constitutes a method specific factor towards biasing city-wide emissions low, which
984 qualitatively counteracts the high bias above. Generally, the tracer method has higher precision
985 than the mobile method, but it is more labor intensive. Although the mobile method has lower
986 precision for emission quantification of individual gas leaks, this method can be implemented
987 widely in a shorter time frame at a city scale. The mobile method is an empirical statistical
988 quantification approach based on controlled release experiments, and a large sample size gives
989 a better estimation in total emission (Weller et al., 2020). Acting on parameters in plume
990 dispersion, such as distance and wind speed which are not included in the method, mobile
991 method can overestimate and underestimate individual gas leaks but with a large number of
992 gas leak quantifications these over- and underestimations may cancel each other out. If (i)
993 particularly large concurrent subsurface CH_4 and C_2H_6 accumulations with multiple emission
994 outlets are observed (this has priority - indication of a large leak) or (ii) a few of the leaks are
995 significantly larger with small subsurface accumulation than the other leaks, an optimal
996 approach may be to supplement the mobile method with use of a more precise measurement
997 method such as the tracer method at those selected locations. The divergence to accurate city-
998 wide quantification is dependent on urban planning, e.g. width of streets, location of gas
999 pipelines (under streets or pavements etc.) and emission outlet location (s).
1000
1001 **4.4 Possible sampling bias of suction method toward low gas leak emission locations**
1002 Following our communications with the emission inventory experts (personal communications
1003 with Christian Böttcher, 2022), we cannot fully reconstruct the methods that are used in the
1004 existing national inventory report to establish the emission factors due to lack of transparency.
1005 However, the German environmental agency (UBA) is considering to use the results of the
1006 recent large scale measurement campaign based on the suction method (MEEM, 2018) in future
1007 publications of the national emission inventory in Germany (Federal Environment Agency,
1008 2021). The utilities choose leak locations for application of the suction method where there are
1009 no safety concerns and/or immediate leak closure is compulsory. This implies that this method
1010 is not applied at locations of the A1 category, which demand immediate repair (P. 27 in MEEM,
1011 2018). Due to logistic constraints and the time-consuming nature of the suction measurements,
1012 they are likely also not (or rarely) applied at locations in the A2 category, which require repair
1013 within a week. Thus, suction measurements have a location sampling bias towards leaks in the
1014 B and C category. This is supported by the fact that the leak locations that were contributed by
1015 the LDC to the intercomparison campaign were locations in the B and C category. This study
1016 investigated whether this location sampling bias could result in an emission rate bias, which
1017 could contribute to the fact that the suction method did not report leaks with emission rates as
1018 high as they have been reported by the mobile method in this study or during previous
1019 measurements in the same city (Maazallahi et al., 2020).
1020 In this study, emission rates from A1 and A2 category leaks were larger compared to those
1021 from B and C category leaks (Figure 6). The emission rate differences vary by measurement
1022 method: a factor 2 for the mobile method (n = 9 for A1&A2, n = 4 for B&C), a factor 11 for
1023 the tracer method (n = 8 for A1&A2, n = 8 for B&C) and a factor 1.6 for the suction method
1024 (n=3 for A1&A2, n = 5 B&C). For the mobile method, there is a clear separation between the
1025 A1&A2 versus the B&C categories. The highest emission estimate for the B&C group
1026 (HH010) is similar to the lowest emission rate estimate for the A1&A2 group (HH014).
1027 Furthermore, HH011 in the A1 category was very likely biased low because of the wrongly
1028 assumed leak location.
1029 For the tracer method, the difference between the two groups is largest, an order of magnitude,
1030 and we know that emissions are underestimated at least at one location of the A1 category

1031 (HH011). The uncertainty of the tracer method is much smaller than the difference between the
1032 two groups. The tracer method also illustrates that 4 of the 5 leaks that were contributed by the
1033 LDC to the intercomparison campaign were extremely small. If these would be representative
1034 for locations where the suction method is usually applied, it would indeed indicate a severe
1035 emission rate bias for the suction method, not because the measurements themselves are biased,
1036 but because locations with low emission rates are targeted with this method. In the
1037 intercomparison campaign, we attempted to apply the suction method also at locations of the
1038 A categories, but at 8 out of 9 locations from the A category, the suction measurements could
1039 not be applied for safety reasons, or suction could not be completed, because of the widespread
1040 subsurface accumulation (Table 2). At the other A location (HH014), the suction method could
1041 not be applied as the ground had been already opened for the repair.
1042

5 Conclusion

1043

1044
1045 In summer 2020, we compared three gas leak rate quantification methods, namely the mobile,
1046 tracer, and suction methods, in Hamburg, Germany. While the mobile and tracer methods have
1047 been compared previously, this is the first peer-reviewed study that includes the suction
1048 method, although suction measurements could not be completed in one day at most locations.
1049 The mobile method can cover large areas in a short time, but some of the smaller leaks (< 0.5
1050 L min^{-1}) are not identified as a gas leak location due to the 10% enhancement threshold in the
1051 standard mobile quantification algorithm. While the mobile method quantification algorithm is
1052 designed to accurately report city-level total gas distribution leak rates (i.e., considering a large
1053 sample size), it has large (known) uncertainties for individual leaks. The tracer method has a
1054 smaller uncertainty, but it is labor intensive in comparison to the mobile method. On average,
1055 CH_4 emissions from natural gas pipeline leaks were higher from mobile quantifications in
1056 comparison to tracer quantifications. For many locations, we encountered several outlets and
1057 with widespread underground gas accumulations. At one location, after deployment of the
1058 mobile and the tracer quantification and during the repair actions, it was found out that the
1059 actual leak in the gas pipeline was located ≈ 60 m away from the identified emission outlet
1060 indicating significant underground gas migration. It is possible that this leak had several
1061 emission outlets that were not identified and the emission quantified from the single outlet is
1062 thus not representative for the whole emission from this leak.
1063 The suction method has a low reported uncertainty, but it is even more labor and time intensive
1064 than the tracer method. Due to the time and effort needed to plan and execute the measurements,
1065 the suction method is likely never applied in routine operation at A1 or A2 safety category
1066 leaks that mandate immediate or near-time repair. In our study, it was also not feasible to apply
1067 the suction method at locations with large subsurface CH_4 accumulations. Our results thus
1068 indicate a systematic difference between A1 and A2 (high emissions) versus B and C (low
1069 emissions) category locations, and generally larger emission rates are inferred with the mobile
1070 and tracer methods for sites with widespread subsurface accumulation.
1071 This study did not allow a direct, quantitative comparison of emission rates estimated with all
1072 three different methods because of the inability to quantify the same leak locations with all
1073 methods. However, this inability illuminates the importance of site selection for deriving
1074 representative emission factors based on empirical measurements. Specifically, the results
1075 suggest that a significant emission rate bias could exist for measurements that are carried out
1076 with the suction method. Our results therefore stipulate that representative site selection
1077 includes sampling at all leak safety categories (MEEM, 2018). Otherwise, this could lead to a
1078 sampling and emission rate bias in the national inventory of gas leak CH_4 emission in Germany.
1079

Authors contributions: TR, HM and SS conceived and designed the study. TR coordinated the campaign in collaboration with DBI, Technical University of Denmark (DTU), Environmental Defense Fund (EDF), E.On and Gasnetz Hamburg (GNH) teams. HM carried out the mobile measurements, emission outlet attribution, performed the analyses of mobile data and collectively with TR analyzed the intercomparison results. AD, CS and AMF performed the tracer method and reported the emission rates from the tracer dataset. HDvdG and TR made instruments and equipment available for the mobile method and CS provided those for the tracer method. HM wrote the paper, and all co-authors supported the interpretation of the results and contributed to improving the paper.

Competing interests: The authors declare that they have no conflict of interest.

Acknowledgement
This study was carried out with the financial support from the Environmental Defense Fund. Extra financial supports were provided by the H2020 Marie Skłodowska-Curie actions through Methane goes Mobile – Measurements and Modelling project (MEMO[2]; https://h2020-memo2.eu/, last access: 20 April 2022), grant number 722479. In this study, Robertson Foundation supported contribution of Stefan Schwietzke. We appreciate efforts from Luise Westphal, Michael Dammann, Ralf Luy, Christian Feickert, Volker Krell, Turhan Ulas, Dieter Bruhns and Sönke Graumann, from GasNetz Hamburg GmbH who facilitated this study by hosting the teams, arranging and applying the carpet method leak detection and confirmation procedures, making information on gas leaks and pipelines available for the data analysis and applying leak repair protocols. We extend our appreciation to Andre Lennartz, Stefan Gollanek and Dieter Wolf from E.On-for their contribution in the planning of the campaign, deploying the suction method at the locations, and exchanging their knowledge and experiences from their previous campaigns. We thank the team from DBI Gas and Environmental Technologies GmbH Leipzig (DBI GUT Leipzig) including Charlotte Große, who contributed to providing information for structuring the campaign planning.

Reference:

Alvarez, R. A., Pacala, S. W., Winebrake, J. J., Chameides, W. L., Hamburg, S. P.: Greater focus needed on methane leakage from natural gas infrastructure, PNAS, 109 (17) 6435-6440, https://doi.org/10.1073/pnas.1202407109, 2012.

Ars, S., Vogel, F., Arrowsmith, C., Heerah, S., Knuckey, E., Lavoie, J., Lee, C., Mostafavi Pak, N., Phillips, J. L., and Wunch, D., Investigation of the Spatial Distribution of Methane Sources in the Greater Toronto Area Using Mobile Gas Monitoring Systems, Environ. Sci. Technol., 54, 24, 15671–15679, https://doi.org/10.1021/acs.est.0c05386, 2020.

Allwine G., Lamb B., Westberg H., Application of Atmospheric Tracer Techniques for Determining Biogenic Hydrocarbon Fluxes from an Oak Forest. In: Hutchison B.A., Hicks B.B. (eds) The Forest-Atmosphere Interaction. Springer, Dordrecht. https://doi.org/10.1007/978-94-009-5305-5_23, 1985.

Arnaldos, J., Casal, J., Montiel, H., Sánchez-Carricondo, M., Vílchez, J.A., Design of a computer tool for the evaluation of the consequences of accidental natural gas releases in distribution pipes, Journal of Loss Prevention in the Process Industries, https://doi.org/10.1016/S0950-4230(97)00041-7, 1998.

Bousquet, P., Ciais, P., Miller, J. B., Dlugokencky, E. J., Hauglustaine, D. A., Prigent, C., Van der Werf, G. R., Peylin, P., Brunke, E. G., Carouge, C., Langenfelds, R. L., Lathière, J., Papa, F., Ramonet, M., Schmidt, M., Steele, L. P., Tyler, S. C., White, J.,

Contribution of anthropogenic and natural sources to atmospheric methane variability. Nature.; 443(7110):439-43. https://doi.org/10.1038/nature05132, 2006.

Brandt, A. R., Heath, G. A., and Cooley, D., Methane Leaks from Natural Gas Systems Follow Extreme Distributions, Environmental Science & Technology, 50 (22), 12512-12520, https://doi.org/10.1021/acs.est.6b04303, 2016

Cho, Y., Ulrich, B. A., Zimmerle, D. J., Smits, K. M., Estimating natural gas emissions from underground pipelines using surface concentration measurements, Environmental Pollution, https://doi.org/10.1016/j.envpol.2020.115514, 2020.

Defratyka, S. M., Paris, J. D., Yver-Kwok, C., Fernandez, J. M., Korben, P., and Bousquet, P., Environmental Science & Technology Article ASAP, https://doi.org/10.1021/acs.est.1c00859, 2021.

Delre, A., Greenhouse gas emissions from wastewater treatment plants: measurements and carbon footprint assessment, Ph.D. Thesis, Department of Environmental Engineering, Technical University of Denmark (DTU), Copenhagen, Available at: https://orbit.dtu.dk/en/publications/greenhouse-gas-emissions-from-wastewater-treatment-plants-measure (Last Accessed: 15 June 2021), 2018.

DVGW: High-performing infrastructure, (2022). [online] Available from https://www.dvgw.de/english-pages/topics/safety-and-security/technical-safety-gas, (Last Accessed: 25 January 2022)

DVGW: Technische Regel-Arbeitsblatt; DVGW G465-1 (A) (2019). [online] Available from: https://shop.wvgw.de/var/assets/leseprobe//510544_lp_G_465-1_2019_05.pdf. (Last Accessed: 15 December 2021)

Ebrahimi-Moghadam, A., Farzaneh-Gord, M., Arabkoohsar, A., Jabari Moghadam, A., CFD analysis of natural gas emission from damaged pipelines: Correlation development for leakage estimation, Cleaner Production, https://doi.org/10.1016/j.jclepro.2018.07.127, 2018.

EC: EU strategy to reduce methane emissionsavailable at: https://eur-lex.europa.eu/legal-content/EN/TXT/?uri=CELEX%3A52020DC0663&qid=1644853088591, (last access: 28 March 2022), 2020

EIA, Carbon Dioxide Emissions Coefficients , available at: https://www.eia.gov/environment/emissions/co2_vol_mass.php, (last access: 28 March 2022), 2021.

EPA, Methane emissions from the natural gas industry: underground pipelines, https://www.epa.gov/sites/production/files/2016-08/documents/9_underground.pdf, 1996.

Federal Environment Agency: National Inventory Report for the German Greenhouse Gas Inventory 1990–2019, available at: https://unfccc.int/documents/194930, (last access: 15 December 2022), 2021.

Fernandez, J. M., Maazallahi, H., France, J. L., Menoud, M., Corbu, M., Ardelean, M., Calcan, A., Townsend-Small, A., van der Veen, C., Fisher, R. E., Lowry, D., Nisbet, E.G., Röckmann, T.: Street-level methane emissions of Bucharest, Romania and the dominance of urban wastewater., Atmospheric Environment: X, 13, 2590-1621, 100153, https://doi.org/10.1016/j.aeaoa.2022.100153, 2022.

Fredenslund, A.M., Scheutz, C., Kjeldsen, P.:. Tracer method to measure landfill gas emissions from leachate collection systems, Waste Management, 30, 2146-2152, https://doi.org/10.1016/j.wasman.2010.03.013, 2010

Fredenslund, A. M., Rees-White, T. C., Beaven, R. P., Delre, A., Finlayson, A., Helmore, J., Allen, G., Scheutz, C.: Validation and error assessment of the mobile tracer gas dispersion method for measurement of fugitive emissions from area sources, Waste Management, 83, 68-78, https://doi.org/10.1016/j.wasman.2018.10.036, 2019.

Federal Environment Agency: National Inventory Report for the German Greenhouse Gas Inventory 1990 – 2018, available at: https://unfccc.int/documents/226313 (last access: 30 March 2022), 2020.

Hendrick, M. F., Ackle, R., Sanaie-Movahed, B., Tang, X., Phillips, N. G., Fugitive methane emissions from leak-prone natural gas distribution infrastructure in urban environments, Environmental Pollution, https://doi.org/10.1016/j.envpol.2016.01.094, 2016.

Hou, Q., Yang, D., Li, X., Xiao, G. and Ho, S. C. M., Modified Leakage Rate Calculation Models of NaturalGas Pipelines, Mathematical Problems in Engineering, https://doi.org/10.1155/2020/6673107, 2020.

Jackson, R. B., Saunois, M., Bousquet, P., Canadell, J. G., Poulter, B., Stavert, A. R., Bergamaschi, P., Niwa, Y., Segers, A. and Tsuruta, A., Increasing anthropogenic methane emissions arise equally from agricultural and fossil fuel sources, Environmental Research Letters, 15, 071002, https://doi.org/10.1088/1748-9326/ab9ed2, 2020.

Jackson, R. B., Down, A., Phillips, N. G., Ackley, R. C., Cook, C. W., Plata, D. L., and Zhao, K., Natural Gas Pipeline Leaks Across Washington, DC, Environ. Sci. Technol., 48, 3, 2051–2058, https://doi.org/10.1021/es404474x, 2014.

Kirchgessner, D. A., Lott R. A., Cowgill, R.M., Harrison, M. R., Shires, T. M., Estimate of methane emissions from the U.S. natural gas industry, Chemosphere, https://doi.org/10.1016/S0045-6535(97)00236-1, 1997.

Keyes, T., Ridge G., Klein, M., Phillips, N., Ackley, R., Yang Y., An enhanced procedure for urban mobile methane leak detection. Heliyon. 9; 6 (10):e04876. https://doi.org/10.1016/j.heliyon.2020.e04876, 2020.

Lamb, B. K., McManus, J. B., Shorter, J. H., Kolb, C. E., Mosher, B., Harriss, R. C., Allwine, E., Blaha, D., Howard, T., Guenther, A., Lott, R. A., Siverson, R., Westburg, H., and Zimmerman, P., Development of atmospheric tracer methods to measure methane emissions from natural gas facilities and urban areas, Environmental Science & Technology 29 (6), 1468-1479 https://doi.org/10.1021/es00006a007, 1995.

Lamb, B. K., Edburg, S. L., Ferrara, T. W., Howard, T., Harrison, M. R., Kolb, C. E., Townsend-Small, A., Dyck, W., Possolo, A., and Whetstone, J. R., Environmental Science & Technology 49 (8), 5161-5169 https://doi.org/10.1021/es505116p, 2015.

Luetschwager, E., von Fischer, J. C., Weller, Z. D., Characterizing detection probabilities of advanced mobile leak surveys: Implications for sampling effort and leak size estimation in natural gas distribution systems. Elementa: Science of the Anthropocene; 9 (1): 00143.https://doi.org/10.1525/elementa.2020.00143, 2021.

Liu, C., Liao, Y., Liang, J., Cui, Z., Li, Y., Quantifying methane release and dispersion estimations for buried natural gas pipeline leakages, Process Safety and Environmental Protection, https://doi.org/10.1016/j.psep.2020.11.031, 2021.

Maazallahi, H., Fernandez, J. M., Menoud, M., Zavala-Araiza, D., Weller, Z. D., Schwietzke, S., von Fischer, J. C., Denier van der Gon, H., and Röckmann, T.: Methane mapping, emission quantification, and attribution in two European cities: Utrecht (NL) and Hamburg (DE), Atmos. Chem. Phys., 20, 14717–14740, https://doi.org/10.5194/acp-20-14717-2020, 2020.

Mahgerefteh, H., Oke, A., Atti, O., Modelling outflow following rupture in pipeline networks, Chemical Engineering Science, https://doi.org/10.1016/j.ces.2005.10.013, 2006.

MEEM, Methane emission estimation method for the gas distribution grid, [Online], Available from: https://www.dbi-gut.de/emissions.html?file=files/PDFs/Emissionen/Final%20Report_MEEM%20DSO_end_signed.pdf&cid=5804. (Last Accessed: 12 December 2022), 2018.

1228 Moloudi, R., Abolfazli Esfahani, J., Modeling of gas release following pipeline rupture:
1229   Proposing non-dimensional correlation, Journal of Loss Prevention in the Process
1230   Industries, https://doi.org/10.1016/j.jlp.2014.09.003, 2014.
1231 Mønster, J. G., Samuelsson, J., Kjeldsen, P., Rella, C. W., Scheutz, C., Quantifying methane
1232   emission from fugitive sources by combining tracer release and downwind
1233   measurements – A sensitivity analysis based on multiple field surveys, Waste
1234   Management,34, 1416-1428, https://doi.org/10.1016/j.wasman.2014.03.025, 2014.
1235 Myhre, G., Shindell, D., Bréon, F. M., Collins, W., Fuglestvedt, J., Huang, J., Koch, D.,
1236   Lamarque, J. F., Lee, D., Mendoza, B., Nakajima, T., Robock, A., Stephens, G.,
1237   Takemura, T., and Zhan, H.: Anthropogenic and Natural Radiative Forc-ing, in:
1238   Climate Change 2013: The Physical Science Basis, Contribution of Working Group I
1239   to the Fifth Assessment Report of the Intergovernmental Panel on Climate Change,
1240   Cambridge,   UK   and   New   York,   NY,   USA,   available   at:
1241   https://www.ipcc.ch/site/assets/uploads/2018/02/WG1AR5_Chapter08_FINAL.pdf,
1242   2013.
1243 Nisbet, E. G., Manning, M. R., Dlugokencky, E. J., Fisher, R. E., Lowry, D., Michel, S. E.,
1244   Myhre, C. L., Platt, S. M., Allen, G., Bousquet, P., Brownlow, R., Cain, M., France, J.
1245   L., Hermansen, O., Hossaini, R., Jones, A. E., Levin, I., Manning, A. C., Myhre, G.,
1246   Pyle, J. A., Vaughn, B. H., Warwick, N. J., White, J. W. C., Very strong atmospheric
1247   methane growth in the 4 Years 2014–2017: implications for the Paris agreement, Global
1248   Biogeochemical Cycles, 33, 318 – 342, https://doi.org/10.1029/2018GB006009, 2019.
1249 Okamoto, H., Gomi, Y., Empirical research on diffusion behavior of leaked gas in the ground,
1250   Journal   of   Loss   Prevention   in   the   Process   Industries,
1251   https://doi.org/10.1016/j.jlp.2011.01.007, 2011.
1252 Phillips, N. G., Ackley, R., Crosson, E. R., Down, A., Hutyra, L. R., Brondfield, M., Karr, J.
1253   D., Zhao, K., Jackson, R. B., Mapping urban pipeline leaks: Methane leaks across
1254   Boston,   Environmental   Pollution,   173,   1-4,
1255   https://doi.org/10.1016/j.envpol.2012.11.003, 2013.
1256 Scheutz, C., Samuelsson, J., Fredenslund, A.M., Kjeldsen, P., Quantification of multiple
1257   methane emission sources at landfills using a double tracer technique, Waste
1258   Management, 31, 1009-1017, https://doi.org/10.1016/j.wasman.2011.01.015, 2011.
1259 Ulrich, B. A., Mitton, M., Lachenmeyer, E., Hecobian, A., Zimmerle, D., and Smits,K. M.,
1260   Natural Gas Emissions from Underground Pipelines and Implications for Leak
1261   Detection, Environmental Science & Technology Letters, 6 (7), 401-406,
1262   https://doi.org/10.1021/acs.estlett.9b00291, 2019.
1263 Von Fischer, J. C., Cooley, D., Chamberlain, S., Gaylord, A., Griebenow, C. J., Hamburg, S.
1264   P., Salo, J., Schumacher, R., Theobald, D., and Ham, J.: Rapid, Vehicle-Based
1265   Identification of Location and Magnitude of Urban Natural Gas Pipeline Leaks,
1266   Environ. Sci. Technol., 51, 4091–4099, https://doi.org/10.1021/acs.est.6b06095, 2017.
1267 Weller, Z. D., Roscioli, J. R., Daube, W. C., Lamb, B. K., Ferrara, T. W., Brewer, P. E., and
1268   von Fischer, J. C.: Vehicle-Based Methane Surveys for Finding Natural Gas Leaks and
1269   Estimating Their Size: Validation and Uncertainty, Environ. Sci. Technol., 52, 11922–
1270   11930, https://doi.org/10.1021/acs.est.8b03135, 2018.
1271 Weller, Z. D., Yang, D. K., and von Fischer, J. C.: An open source algorithm to detect natural
1272   gas leaks from mobile methane survey data, edited by: Mauder, M., PLoS One, 14,
1273   e0212287, https://doi.org/10.1371/journal.pone.0212287, 2019.
1274 Weller, Z. D., Hamburg, S. P., and von Fischer, J. C., A National Estimate of Methane Leakage
1275   from Pipeline Mains in Natural Gas Local Distribution Systems, Environmental
1276   Science & Technology, 54 (14), 8958-8967, https://doi.org/10.1021/acs.est.0c00437,
1277   2020

1278 Wiesner, S., Gröngröft, A., Ament, F. et al. Spatial and temporal variability of urban soil water
1279   dynamics observed by a soil monitoring network. J Soils Sediments 16, 2523–2537.
1280   https://doi.org/10.1007/s11368-016-1385-6, 2016
1281 Worden, J. R., Anthony Bloom, A., Pandey, S., Jiang, Z., Worden, H. M., Walker, T. W.,
1282   Houweling, S., Röckmann, T., , Reduced biomass burning emissions reconcile
1283   conflicting estimates of the post-2006 atmospheric methane budget, Nature
1284   Communications 8, 2227 https://doi.org/10.1038/s41467-017-02246-0, 2017
1285 Yan, Y., Dong, X., Li, J., Experimental study of methane diffusion in soil for an underground
1286   gas pipe leak, Journal of Natural Gas Science and Engineering,
1287   https://doi.org/10.1016/j.jngse.2015.08.039, 2015.
1288 Yuhua, D., Huilin, G., Jing'en, Z., Yaorong, F., Evaluation of gas release rate through holes in
1289   pipelines, Journal of Loss Prevention in the Process Industries,
1290   https://doi.org/10.1016/S0950-4230(02)00041-4, 2002.
1291